Crustal structure of the conjugate Equatorial Atlantic Margins, derived by gravity anomaly inversion

NICK J. KUSZNIR[1,2], ALAN M. ROBERTS[2]* & ANDREW D. ALVEY[2]

[1]*Department of Earth & Ocean Sciences, University of Liverpool, Liverpool L69 3BX, UK*

[2]*Badley Geoscience Ltd, North Beck House, North Beck Lane, Spilsby, Lincolnshire, PE23 5NB, UK*

A.M.R., 0000-0003-4839-0741

Correspondence: alan@badleys.co.uk

Abstract: The crustal structure of the Equatorial Atlantic conjugate margins (South America and West Africa) has been investigated using 3D gravity anomaly inversion, which allows for (1) the elevated geothermal gradient of the lithosphere following rifting and break-up and (2) magmatic addition to the crust during rifting and break-up. It is therefore particularly suitable for the analysis of rifted margins and their associated ocean basins. Maps of crustal thickness and conjugate-margin stretching, derived from gravity anomaly inversion, are used to illustrate how the Equatorial Atlantic opened as a set of stepped rift-transform segments, rather than as a simple orthogonal rifted margin. The influence of the transform faults and associated oceanic fracture zones is particularly clear when the results of the gravity anomaly inversion are combined with a shaded-relief display of the free-air gravity anomaly. A set of crustal cross-sections has been extracted from the results of the gravity inversion along both equatorial margins. These illustrate the crustal structure of both rifted-margin segments and transform-margin segments. The maps and cross-sections are used to delineate crustal type on the margins as (1) inboard, entirely continental, (2) outboard, entirely oceanic and (3) the ocean–continent transition in between where mixed continental and magmatic crust is likely to be present. For a given parameterization of melt generation the amount of magmatic addition within the ocean–continent transition is predicted by the gravity inversion. One of the strengths of the gravity-inversion technique is that these predictions can be made in the absence of any other directly acquired data. On both margins anomalously thick crust is resolved close to a number of oceanic fracture zones. On the South American margin we believe that this thick crust is probably the result of post-break-up magmatism within what was originally normal-thickness oceanic crust. On the West African margin, however, three possible origins are discussed: (1) continental crust extended oceanwards along the fracture zones; (2) oceanic crust magmatically thickened at the fracture zones; and (3) oceanic crust thickened by transpression along the fracture zones. Gravity inversion alone cannot discriminate between these possibilities. The cross-sections also show that, while 'normal thickness' oceanic crust (*c.* 7 km) predominates regionally, local areas of thinner (*c.* 5 km) and thicker (*c.* 10 km) oceanic crust are also present along both margins. Finally, using maps of crustal thickness and thinning factor as input to plate reconstructions, the regional palaeogeography of the Equatorial Atlantic during and after break-up is displayed at 10 Ma increments.

Supplementary material: Detailed illustrations of the crustal-thickness mapping, the crustal cross-sections and the plate reconstructions are available at: https://doi.org/10.6084/m9.figshare.c.4031266.v1

Gravity anomaly inversion is an excellent entry point into the analysis of rifted continental margins at the regional scale. Much, often all, of the required input information is available in the public domain, enabling geologically consistent analysis of large areas to be performed. Other techniques may provide more detailed information on a more local scale (e.g. Fletcher *et al.* 2013; Roberts *et al.* 2013; Cowie *et al.* 2015, 2016), but at the regional scale gravity anomaly inversion is the best starting point, not least because full data coverage is available for oceanic areas as well as for the continental margins themselves.

In this paper we take advantage of complete data coverage across the Atlantic to investigate the crustal structure of the conjugate margins of equatorial South America and West Africa, together with their linkage across the Atlantic ocean. The results were originally compiled as input to an industry workshop discussing the exploration potential of the Equatorial Atlantic (PESGB 2016). Significant hydrocarbon discoveries exist on both margins but their potential is not yet thought to be exhausted. Analysis of crustal basement structure, with its associated implications for basement heat flow (e.g. Cowie & Kusznir 2012*a*), is likely to be an

important part of any future exploration screening strategy in these areas.

The gravity inversion technique applied to derive crustal structure has been described in several previous publications (e.g. Greenhalgh & Kusznir 2007; Alvey *et al.* 2008; Chappell & Kusznir 2008; Cowie & Kusznir 2012b; Roberts *et al.* 2013; Cowie *et al.* 2015) and so is recapped here only briefly. In Roberts *et al.* (2013) and Cowie *et al.* (2015, 2016) gravity inversion has been used alongside other techniques, such as subsidence analysis and analysis of residual depth anomalies, to provide a multifaceted view of rifted margin structure. Here, however, we wish to focus on what gravity inversion alone can provide, while recognizing that its use alongside other techniques can, of course, provide yet more information.
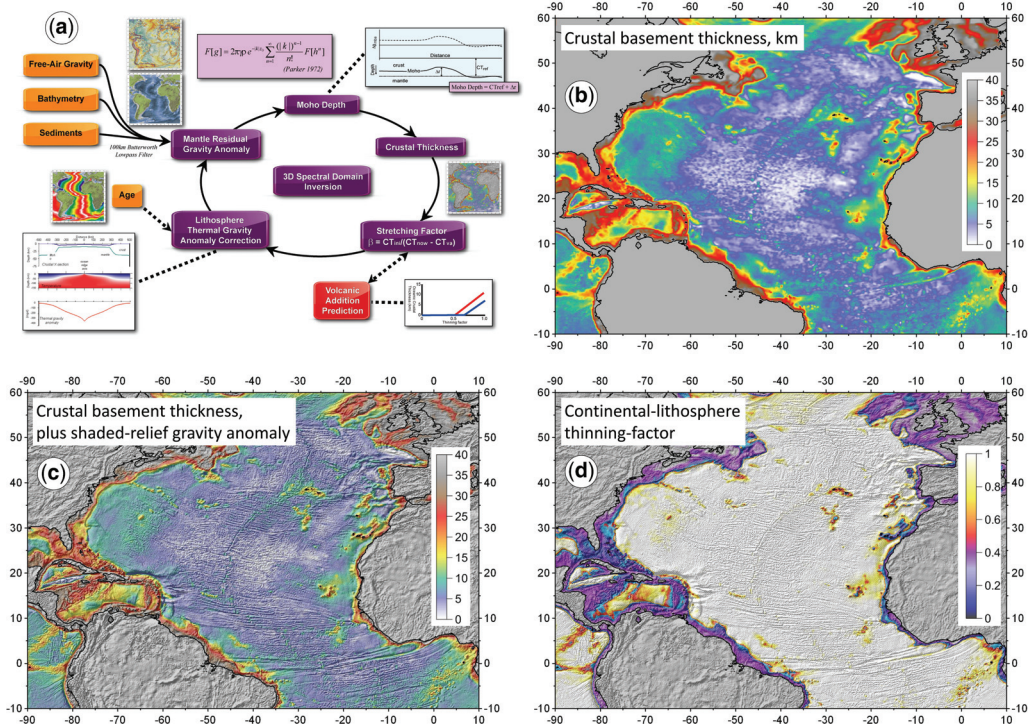
3D gravity inversion method

The gravity inversion method and workflow are summarized in Figure 1a (adapted from Alvey

2010; Roberts *et al.* 2013). The three principal sets of input data are maps/grids of:

- satellite free-air gravity anomaly data (Sandwell & Smith 2009 and subsequent updates at http://topex.ucsd.edu/WWW_html/mar_grav.html);
- bathymetric/topographic data (Smith & Sandwell 1997 and subsequent updates at http://topex.ucsd.edu/WWW_html/mar_topo.html);
- sediment thickness data (e.g. Laske & Masters 1997 and subsequent updates at http://igppweb.ucsd.edu/~gabi/sediment.html; and Divins 2003 and subsequent updates at http://www.ngdc.noaa.gov/mgg/sedthick/sedthick.html).

Each of these cited datasets is freely and publicly available. Public-domain sediment thickness information can be replaced by proprietary information for a particular area, should such information exist. Use of such proprietary sediment thickness information will almost certainly improve the reliability of the results for a study with local focus. For

Fig. 1. (**a**) Schematic outline of the gravity inversion methodology to determine Moho depth, crustal basement thickness and lithosphere thinning factor, using gravity anomaly inversion incorporating a lithosphere thermal correction and decompression-melt prediction. Adapted from Alvey (2010) and Roberts *et al.* (2013). (**b**) Example map of total crustal basement thickness (continental and oceanic) produced by gravity inversion of the offshore central Atlantic region. Scale in kilometres. (**c**) Map of total crustal basement thickness (as in b) overlain by a display of the shaded-relief free-air gravity anomaly. The overlay helps to delineate major tectonic features within the results. Scale in kilometres. (**d**) Example map of continental-lithosphere thinning factor $(1 - 1/\beta)$ for the central Atlantic, overlain by the shaded-relief free-air gravity anomaly.

regional-scale analysis, however, and for coverage into the oceans, the global public sources are generally required.

The principal output from the gravity inversion comprises maps of:

- present-day depth to Moho, the primary output on which all other results are based (Fig. 1a);
- total crustal basement thickness (base sediment to Moho, no distinction between continental and oceanic crust);
- residual thickness of the continental crust (total crustal basement thickness minus predicted volcanic addition, see below); and
- lithosphere stretching factor (β) and thinning factor (γ), where $\gamma = 1 - 1/\beta$.

Where public-domain sediment thickness information can be calibrated against estimates of sediment thickness from good-quality seismic-reflection data we find, both in the Equatorial Atlantic area and elsewhere, that the public-domain data tend to underestimate the sediment thickness. The consequence of this in a regional gravity inversion study, as described here, is that estimates of crustal thickness will be a probable maximum and estimates of stretching/thinning will be a probable minimum.

Key to the success of the gravity inversion method employed in this paper is a correction for the gravity anomaly associated with the elevated geotherm within both continental-margin and oceanic lithosphere which results from rifting/break-up of the margin and the formation of an ocean basin. The lithosphere thermal gravity anomaly is negative and very large ($c. -350$ mgal at a young ocean ridge). Failure to include a correction for the lithosphere thermal gravity anomaly leads to a substantial over-estimate of Moho depth and crustal basement thickness and an under-estimate of continental-lithosphere thinning. The magnitude of the gravity anomaly decreases with time as the thermal anomaly cools following rifting/break-up but for a mid-Cretaceous break-up age, as in the case of the Equatorial Atlantic, it is essential to include the lithosphere thermal gravity anomaly correction. The methodology by which the thermal gravity anomaly correction is included in the gravity inversion is described in detail in Chappell & Kusznir (2008, see also Fig. 1a).

The gravity inversion method that we use determines Moho depth and crustal basement thickness but cannot itself distinguish between continental and oceanic crust. In order to differentiate oceanic crust from continental-basement crust we use a parameterization of decompression melting. Following McKenzie & Bickle (1988) and White & McKenzie (1989) it is assumed that decompression melting of the lithosphere occurs at high continental-lithosphere thinning and stretching factors, resulting in magmatic addition which contributes to the total thickness of the crust (Chappell & Kusznir 2008, fig. 3, see also Fig. 1a). As stretching proceeds beyond a given critical value the original continental crust will continue to stretch and thin, but the total thickness of the crust will be buffered by the addition of new magmatic material. Thus, following magmatic addition, the location of the base of the crust (Moho) is controlled both by the magnitude of stretching/thinning of the continental crust and by the amount of newly added magmatic material.

Using the central Atlantic as an illustration, Figure 1b–d shows how the results of the gravity inversion are compiled to reveal geological information in map form. The specific parameters constraining the inversion are not described at this point, but will be returned to later in the paper when detail of the equatorial region is discussed. Figure 1b shows a map of crustal thickness (Moho to base sediment) for the central Atlantic (offshore regions only). There is no distinction in this map between areas of predicted continental crust and oceanic crust. Thick crust is seen at the continental margins and within internal basins beyond the margins. Thin crust is seen in the centre of the Atlantic.

While Figure 1b illustrates the basic result of the gravity inversion, the information conveyed by this map can be greatly enhanced by adding an overlay of the shaded-relief free-air gravity anomaly (Fig. 1c), which is the gravity anomaly data used as input to the inversion. This additional information allows us to pick out features such as the mid-ocean ridge, transform faults and tectonic flowlines within the oceanic area and immediately aids the understanding of margin conjugacy. Within the paper all future results in map form are shown with an overlay of shaded-relief free-air gravity anomaly.

Figure 1d shows the map of continental-lithosphere thinning factor which results from the map of crustal thickness once the correction for volcanic addition is taken into account. A thinning factor value of 0 is no continental thinning. A value of 1 is complete thinning and removal of the continental crust and continental lithosphere. As expected, gradations in thinning factor occur across the continental margins on both sides of the Atlantic, while the large white area in the centre of the map corresponds to a thinning factor of 1 and the presence of oceanic crust. There are other maps from the gravity inversion which can be displayed, some of which are shown later, but the specific objective of Figure 1 is to introduce the technique. The technique itself has acquired the acronym of OCTek Gravity Inversion, derived from its focus on the tectonics of the ocean–continent transition (OCT).

A global compilation of crustal thickness

Figure 1, in common with all previous published maps derived from the OCTek gravity inversion

technique (see references above), shows results only in offshore areas. This is not a technical restriction of the technique itself, but has come about because public-domain sediment-thickness information in offshore areas tends to be of better quality and more reliable than it is onshore. In particular the Divins (2003) data is higher resolution than the older Laske & Masters (1997) data, but it is only available offshore, whereas the Laske & Masters data has global offshore and onshore coverage at a coarse resolution of 1 × 1°. If the coarseness of this coverage can be accepted then the gravity inversion technique can be extended onshore.

Figure 2 shows, in a series of four 90° rotations, a global map of crustal basement thickness, derived from the OCTek gravity inversion technique. We believe that the first-order results, in terms of identifying areas of thick crust, thin crust and transition in between, will be correct in both onshore and offshore areas. We would advise caution, however, in taking the onshore crustal-thickness values too literally against the scale provided because of (1) the variability in the quality of the underlying sediment-thickness information and (2) uncertainties in parameterizing both break-up/rift ages (where appropriate) and magmatic addition from decompression melting.
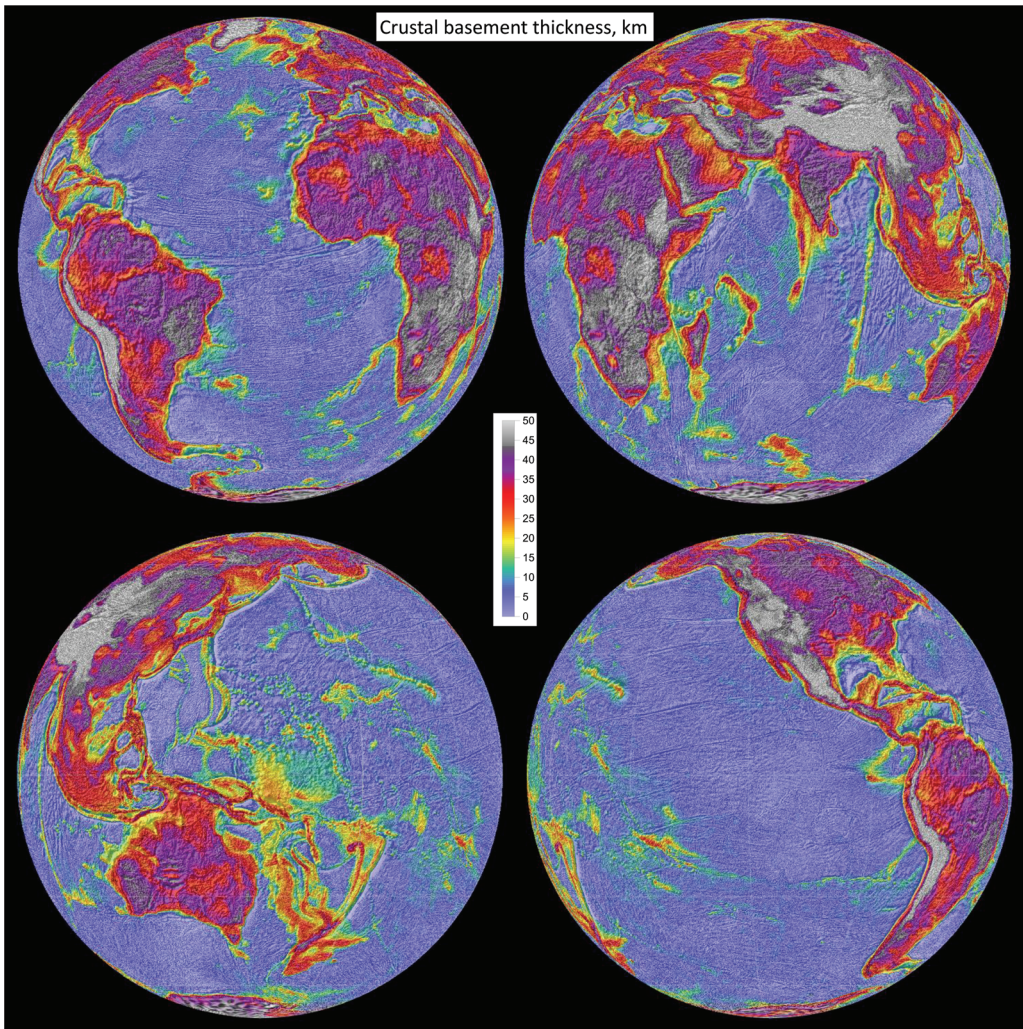
Fig. 2. Four maps, at 90° rotation increments, showing global, total crustal basement thickness (continental and oceanic) derived by OCTek gravity inversion. Scale in kilometres. Both onshore and offshore regions are included for the first time in such results.

The importance of being able to map crustal thickness at any location and overlay the results with tectonic information from the shaded-relief gravity anomaly is that this provides us with a window into areas in which little or no direct geological information has been acquired, specifically offshore deep-water areas with no seismic reflection data, seismic refraction data or drilling information. The thickness of continental crustal basement controls the crustal radiogenic heat input into a basin (e.g. Cowie & Kusznir 2012a). An understanding of crustal-thickness distribution and crustal composition therefore provides information which is essential for the prediction of basement heat flow, an important input to petroleum-systems analysis.

In the rest of the paper we will focus on a smaller area within Figure 2 but a large area in its own right, the Equatorial Atlantic.

Crustal thickness across the Equatorial Atlantic

Figure 3 shows a map of crustal basement thickness for the Equatorial Atlantic, extending north into the Central Atlantic and south into the South Atlantic. Crustal thickness for both onshore and offshore areas is included and the map itself is an extraction from Figure 2. There is no differentiation between continental and oceanic crust in this map, it is simply predicted crustal basement thickness. The gravity inversion results shown in Figure 3 are tuned to a break-up age of 110 Ma and are applicable to the Equatorial Atlantic. Other more specific input data and parameters are described below in the context of Figures 4 and 5.

In the onshore areas of South America and Central/North Africa, Figure 3 picks out areas of localized thinner crust (20–30 km) within the
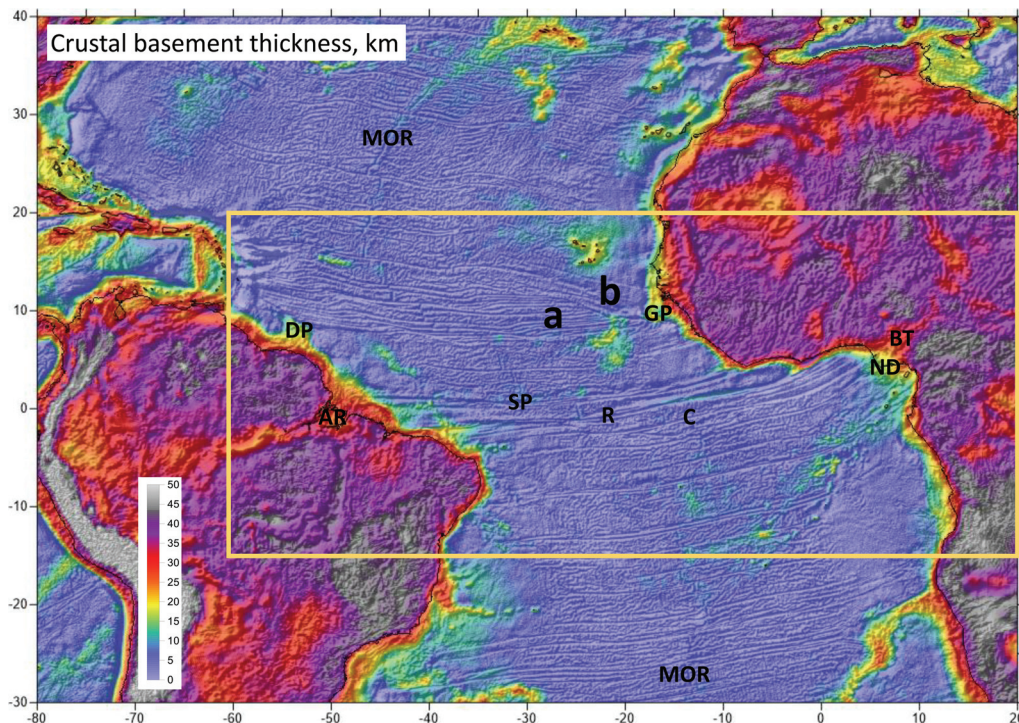
Fig. 3. Map of total crustal basement thickness (continental and oceanic) from gravity inversion of the Equatorial Atlantic, overlain by a display of the shaded-relief free-air gravity anomaly. Scale in kilometres. For regional clarity the map also extends north into the Central Atlantic and south into the South Atlantic. The focus of the main equatorial study is shown by the outline box. **a** identifies an area of prominent *c.* east–west oceanic fracture-zone flowlines related to Cretaceous opening of the Equatorial Atlantic. **b** identifies an area of clockwise-oblique fracture-zone flowlines related to the earlier Jurassic opening of the Central Atlantic. MOR, mid-ocean-ridge; DP, Demerara Plateau; GP, Guinea Plateau; AR, Amazon Rift; BT, Benue Trough; ND, Niger Delta; SP, St Paul's fracture zone; R, Romanche fracture zone; C, Chain fracture zone. (A higher-resolution display of the same map is available within Supplementary Material, Figure S1.)
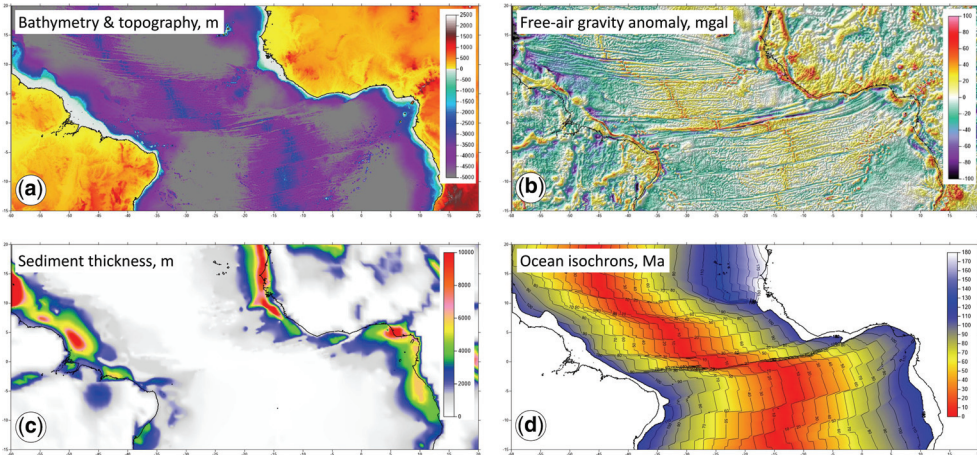
Fig. 4. Primary input data for gravity inversion of the Equatorial Atlantic. (**a**) Bathymetry and topography, scale in metres (Smith & Sandwell 1997 and updates). (**b**) Satellite free-air gravity anomaly, scale in mgal (Sandwell & Smith 2009 and updates), overlain by a shaded-relief display of itself. (**c**) Sediment thickness, scale in metres (Divins 2003 offshore; Laske & Masters 1997 onshore). (**d**) Ocean isochrons, scale in millions of years (Müller *et al.* 2008), used to determine the age of the lithosphere thermal-gravity anomaly in oceanic areas.
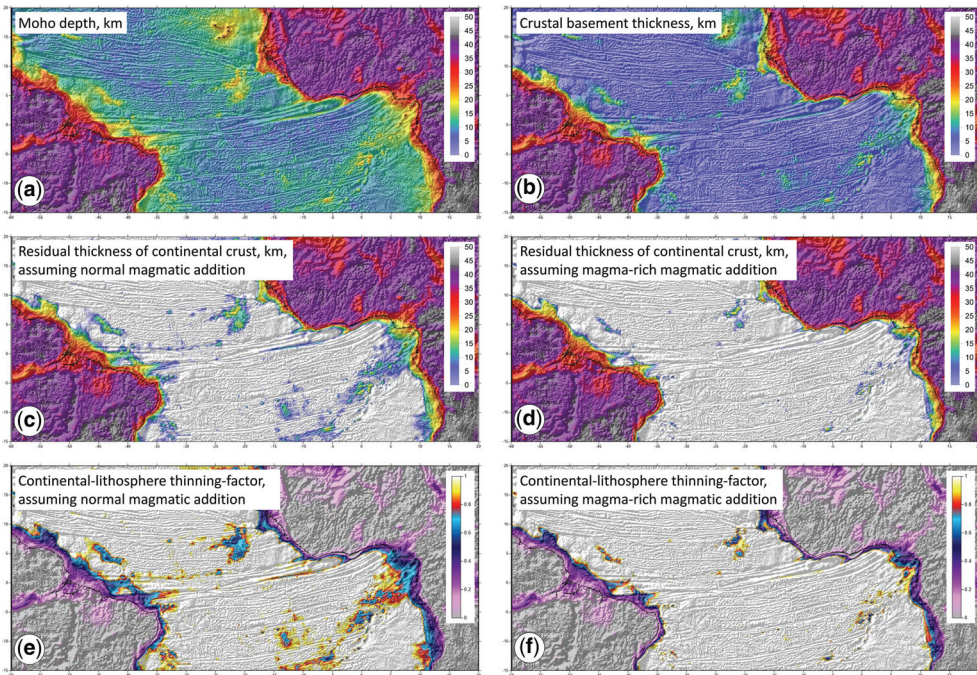
Fig. 5. Results from two gravity inversion models for the Equatorial Atlantic, one assuming 'normal' magmatic addition (decompression melting), the other assuming 'magma-rich' magmatic addition. Both models use a break-up age of 110 Ma and a Reference Moho Depth of 37.5 km. (**a**) Moho depth, common to both models. (**b**) Total crustal basement thickness (continental and oceanic), common to both models. (**c**) Residual thickness of the continental crust, assuming normal magmatic addition. (**d**) Residual thickness of the continental crust, assuming magma-rich magmatic addition. (**e**) Continental-lithosphere thinning factor $(1 - 1/\beta)$, assuming normal magmatic addition. Thinning factor 1 defines oceanic crust. (**f**) Continental-lithosphere thinning factor, assuming magma-rich magmatic addition. Scale in kilometres for Moho depth and crustal basement thickness.

broader cratonic areas where the crust is 40 km or more in thickness. The thinner areas correspond to known onshore rifts, perhaps the most obvious of which are the Amazon rift and the Benue Trough (Fig. 3). Some of these onshore rifts in the equatorial region are older than the Cretaceous break-up of the Atlantic margins and can be matched across the two continents by plate restoration (see later in this paper). We reiterate the point made above not to take the onshore crustal-thickness values too literally against the scale provided, but rather consider the first-order results in terms of mapped crustal thickness variations.

At the scale of Figure 3 the gradation from thick crust onshore to thin crust in the offshore oceanic areas is rapid. These are the areas of the stretched and thinned continental margins, details of which are investigated in the subsequent discussion which follows.

Within the broad oceanic area itself the crust has a thickness of *c.* 7 km (normal thickness oceanic crust), with the exception of localized volcanic seamounts and seamount chains, which map as areas of thicker crust (10–20 km). The shaded-relief gravity adds detail to the oceanic areas which would not otherwise be apparent. The Atlantic mid-ocean ridge is clearly picked out. So too is its far-from-linear structure; it is offset by many small and large fracture zones/transform faults. This is particularly apparent across the prominent fracture zones of the equatorial area.

The fracture zones also allow us to identify the flowlines which define plate-separation direction over time. In the area labelled (a) the broadly east–west flowlines of separation in the Cretaceous and younger (110 Ma onwards) oceanic crust can be seen as a strong imprint across most of the ocean width (see also isochrons in Fig. 4). Just to the north of (a), however, in the area labelled (b), the flowlines strike clockwise of east–west with a clear angular discordance where the two sets meet. The flowlines at (b) relate to the earlier Jurassic opening of the Central Atlantic between North Africa and North America (see isochrons in Fig. 4). This initial Jurassic opening of the Central Atlantic occurred in a direction *c.* 10° clockwise to the younger Cretaceous opening further south. The adjustment within the older Jurassic oceanic segment to the younger opening direction can be seen in the curve of the flowlines west of (b).

Conditioning the Equatorial Atlantic gravity inversion

Figures 4 and 5 illustrate the data input and model parameterization used for gravity inversion of the Equatorial Atlantic. Figure 4a shows the bathymetry and topography data for the equatorial region (Smith & Sandwell 1997 & updates). Figure 4b shows the free-air gravity anomaly data (Sandwell & Smith 2009 & updates) overlain by a shaded-relief display of itself. Figure 4c shows the sediment thickness data used in the gravity inversion, which is a merge of Divins (2003) offshore and Laske & Masters (1997) onshore. As expected, the thickest sediments are concentrated along the continental margins. As mentioned above, this compilation of public-domain data is likely to provide a minimum estimate of sediment thickness at the regional scale. Figure 4d shows the ocean isochrons (Müller *et al.* 2008) for the Equatorial Atlantic.

An area for which the public-domain sediment-thickness information (Fig. 4c) is known to be an under-estimate is the Niger Delta (Fig. 3). Here the gravity inversion shows the delta lying on thinned continental crust (Figs 3, 5 & 8a), in an area where the basement is known to be oceanic (see the ocean isochrons in Fig. 4d).

The ocean isochrons are required in order for the gravity inversion to work correctly in areas of known oceanic crust. In the Equatorial and South Atlantic the oceanic crust spans the age range 110 Ma to present. To the north, in the Central Atlantic, the age range is 180 Ma to present. The age of inception of the lithosphere thermal-gravity anomaly in the oceanic areas varies with the age of the ocean crust. This results in a spatially varying lithosphere thermal-gravity anomaly at the present day: very large at the mid-ocean ridge (*c.* 350 mgal) and much lower (*c.* 50 mgal or less) at the oldest oceanic lithosphere and at the rifted margins. Ocean isochrons are used to give the thermal re-equilibration time (cooling time) of the lithosphere thermal anomaly within the oceanic areas and thus produce gravity inversion results (e.g. Moho depth, crustal thickness, Fig. 3) that fully compensate for the underlying oceanic thermal structure.

In order to condition the lithosphere thermal-gravity anomaly across the rifted continental margins of West Africa and South America, a fixed break-up age is used for the lithosphere thermal re-equilibration time within the continental region and for the region of uncertain crustal affinity across the OCT. In the Equatorial Atlantic region (Fig. 4) this age is 110 Ma. Further to the north in the Central Atlantic (Fig. 3) it is 170 Ma.

Figure 5 shows a set of results from two gravity inversion models of the Equatorial Atlantic. Both models have used all of the input data in Figure 4, a break-up age of 110 Ma and a Reference Moho Depth of 37.5 km. Reference Moho Depth is a geophysical/geodetic parameter that represents the reference datum to which Moho relief determined by gravity inversion is applied in order to determine Moho depth. It is controlled by the long-wavelength

component of the Earth's gravity field which results from deep (sublithosphere) mantle processes and structure (see Cowie & Kusznir 2012b; Cowie et al. 2015 for more detailed discussions).

Where the two inversion models of Fig. 5 differ is in their parameterization of magmatic addition. The model results shown in Figure 5c and e correspond to decompression melting assuming 'normal' magmatic addition, in which melting begins at thinning factor 0.7 and produces 7 km of oceanic crust when thinning factor reaches 1. This is the parameterization of melting for normal temperature asthenosphere (McKenzie & Bickle 1988; White & McKenzie 1989) first applied by Chappell & Kusznir (2008). The results shown in Figure 5d and f use decompression melting assuming 'magma-rich' magmatic addition, in which melting begins at thinning factor 0.5 and produces 10 km of oceanic crust when thinning factor reaches 1 (Fig. 1a, Chappell & Kusznir 2008 fig. 3; Roberts et al. 2013 fig. 1b). The gravity inversion method can parameterize any combination of critical thinning factor and magmatic addition, but here we concentrate on the base-case 'normal' model and an enhanced 'magma-rich' case.

The results of the gravity inversion for both Moho depth and total crustal basement thickness are largely insensitive to the parameterization of magmatic addition and thus the maps in Figure 5a and b are common to both models. Residual thickness of the continental crustal basement (Fig. 5c, d) and lithosphere thinning factor (Fig. 5e, f) are, however, both sensitive to magmatic addition and thus Figure 5c and e are different to 5d and f.

Maps of the residual thickness of the continental crust (Fig. 5c, d) are produced by subtracting the magmatic addition predicted within the gravity inversion from the calculated total crustal thickness. In oceanic areas this therefore results in a prediction of zero thickness for remaining continental crust (white in Fig. 5c, d). When comparing Figure 5c and d the difference is most apparent within the oceanic area, where the allowance for greater magmatic addition in Figure 5d 'cleans up' some of the areas of oceanic crust over-thickened by seamounts. There is, however, also a more subtle difference (at the scale of the current maps) across the area of the outer continental margin where the prediction of greater magmatic addition in Figure 5d results in thinner continental crust and a shift inboard of the continent–ocean boundary (COB; edge of oceanic white zone). This can be made clearer when the maps for a particular area are enlarged.

Maps of thinning factor ($1 - 1/\beta$, Fig. 5e, f) are produced by comparing the thickness of the residual continental crust (Fig. 5c, d) with the assumed initial thickness of the continental crust, which in the equatorial area is 37.5 km. Where the predicted thickness of continental crust is 37.5 km or greater the thinning factor is 0. Where the thickness of continental crust is zero (oceanic), the thinning factor is 1. Figures 5e and f differ from each other in the same areas and for the same reasons as Figures 5c and d, with oceanic areas again being displayed as white.

In the absence of any information to the contrary, 'normal' magmatic addition should generally be considered the base case in any particular area. The most straightforward calibration of magmatic addition can be obtained using Moho depth from deep, long-offset seismic reflection data which extends on to known oceanic crust, in which case magmatic addition in the gravity inversion can be calibrated by the thickness of the oldest oceanic crust. Under 'normal' conditions this will be c. 7 km and as calibration examples later in the paper show, this is probably the general case for the Equatorial Atlantic. The North American side of the Central Atlantic to the immediate north (Fig. 3), however, is known to show characteristics of a 'magma-rich' margin (Eldholm et al. 2000) and thus 'normal' and 'magma-rich' solutions are presented in Figure 5.

Following from the discussion of magmatic addition, Figure 6 (adapted from Manatschal et al. 2015) reminds us that rifted continental margins should not simply be considered as the two magmatic cases covered by the models in Figure 5. At one end of the 'magmatic scale' lie 'magma-poor' margins with little or no magmatic addition at the time of break-up (Fig. 6a). Magma-poor margins result in mantle exhumation rather than the formation of new oceanic crust. At the other end of the scale lie 'magma-rich' margins, with enhanced volcanic addition producing extrusive lavas and seaward-dipping reflectors, in addition to thick (c. 10 km) oceanic crust (Fig. 6b). In between these two end members lies a complete range which may be encountered in natural examples. It is within this range that margins approaching the 'normal' case will be the most common, but even within relatively local areas some variation in magmatic addition can be expected.

Crustal structure of the South American equatorial margin

Figure 7a shows a map of total crustal basement thickness for the South American equatorial margin, enlarged from Figures 3 and 5a. This result is independent of magmatic addition, because it does not differentiate between continental and oceanic crust. The regional strike of both the Atlantic ocean margin and the South American coast in this area is NW–SE, at c. 45° to the opening direction of the Atlantic as defined by the east–west-aligned fracture zones. The coast and margin are not orthogonal to the opening direction because this is not a simple, linear rifted margin. Rather the margin is subdivided into a
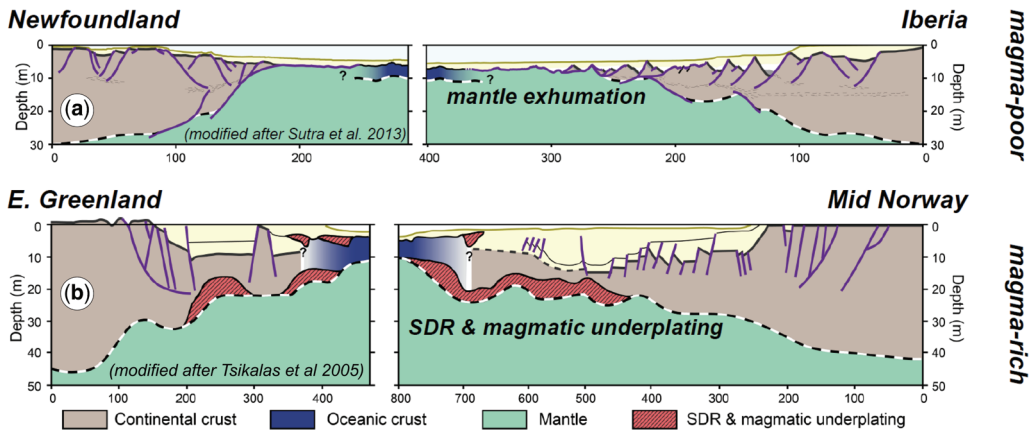
Fig. 6. Example cross-sections of end-member margin types showing: (**a**) the conjugate magma-poor margins of Newfoundland and Iberia; (**b**) the conjugate magma-rich margins of East Greenland and Norway. (Adapted from Manatschal *et al.* 2015 fig. 2 by Gianreto Manatschal and used with permission. Original sources Tsikalas *et al.* 2005; Sutra *et al.* 2013.)

number of relatively short rift segments (margin strike north–south) and transform segments (margin strike east–west) by the numerous oceanic fracture zones, which give the margin a stepped, oblique regional geometry. Figure 3 shows that the fracture zones are easily correlatable across to the African margin, which has a similar stepped rift/transform geometry (Fig. 8a). The well-known St Paul's, Romanche and Chain fracture zones are each identified in Figures 3, 7a and 8a.

Figure 7b comprises 15 crustal-scale cross-sections extracted from the results of the gravity inversion (Fig. 7a). The cross-sections are constructed from four key geological surfaces, two of which are input to the gravity inversion and two of which are results. The input surfaces are seabed/bathymetry (plus topography in onshore areas) and the base sediment (Divins 2003 offshore; Laske & Masters 1997 onshore). Together these two surfaces define the sediment thickness. The output surfaces are Moho depth (Fig. 5a) and the top of magmatic addition (see below).

The area between the Moho and base sediment defines the total crustal basement thickness in both continental and oceanic areas (Figs 3 & 7a). The area between the top of magmatic addition and the Moho defines the amount of magmatic addition predicted by the gravity model. The distribution of magmatic addition is then used in turn to define the three main crustal zones of the margin:

(1) inboard areas with no magmatic addition, where the crustal basement is entirely continental – the Moho and top of magmatic addition are here coincident in the cross-sections;

(2) outboard areas where the continental crust has been entirely replaced by magmatic addition and crustal basement is entirely oceanic – the base sediment and top of magmatic addition are here coincident in the cross-sections;

(3) the area between 1 and 2 comprising the OCT, where both highly thinned continental crust and new magmatic addition are likely to be present – in this area the top of magmatic addition is a distinct interface in the cross-sections.

Within the area of the OCT on the cross-sections, where continental and magmatic crust are both present, the new magmatic addition is displayed as underlying the thinned continental crust with an 'underplating' geometry. This is simply a graphical construction within the cross-sections and no specific volcanic mechanism or location is implied. The magmatic addition in each case could be a combination of underplating, intrusion and extrusion, but it is represented for simplicity on the cross-sections as a new layer underlying the thinned continental crust. This construction produces a typical 'feather-edge' geometry to the continental crust as it thins to zero and is replaced by oceanic crust.

The 15 cross-sections have been constructed so that some are orientated *c.* east–west, lying along the opening direction of the Equatorial Atlantic (i.e. they are dip lines). These sections define the crustal geometries of the rift segments to the margin. Others are orientated *c.* north–south and define the crustal geometries of the transform segments. Possible exceptions to this are cross-sections 1 and 2, in the NW corner of the map (Fig. 7a) and lying to the NW of the Demerara Plateau. These two sections
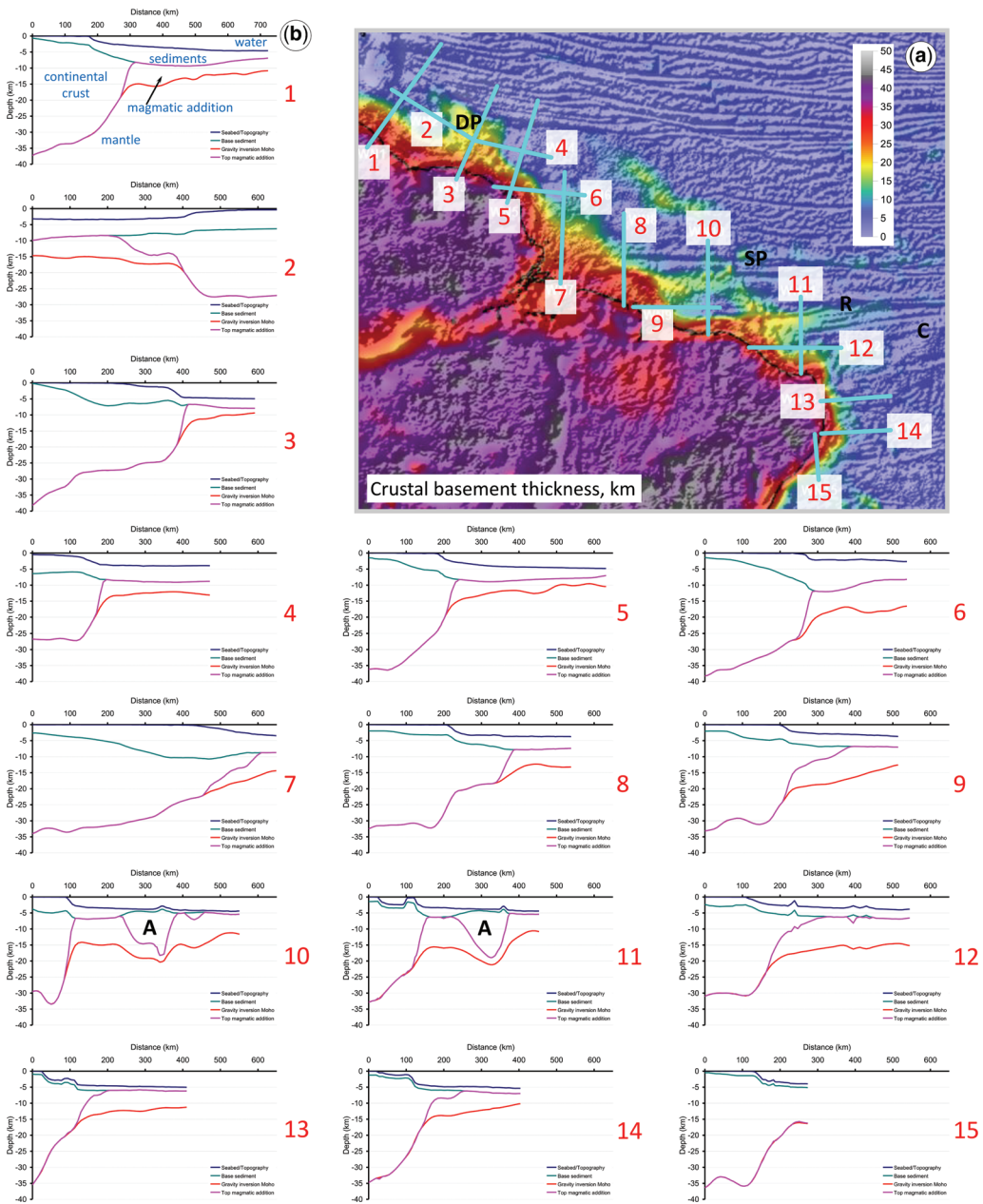
Fig. 7. (**a**) Map of total crustal basement thickness for the South American equatorial margin, enlarged from Figure 5a. Scale in kilometres. DP, Demerara Plateau; SP, St Paul's fracture zone; R, Romanche fracture zone; C, Chain fracture zone. The locations of the 15 cross-sections comprising (b) are shown. (**b**) Fifteen crustal-scale cross-sections extracted from the results of the gravity inversion. Sections 1 and 2 use a Jurassic break-up age of 170 Ma. Sections 3–15 use a Cretaceous break-up age of 110 Ma. Sections 1–5, 7, 8 and 13–15 were determined assuming 'normal' magmatic addition. Sections 6, 9–12 were determined assuming 'magma-rich' magmatic addition. Sections 1, 4, 5, 9 and 12–14 cross rifted margin segments. Sections 2, 3, 6–8, 10, 11 and 15 cross transform margin segments. On sections 10 and 11 A indicates areas of anomalously thick crust outboard of the COB (see text). (A higher-resolution display of the same cross-sections is available within Supplementary Material, Figure S1.)
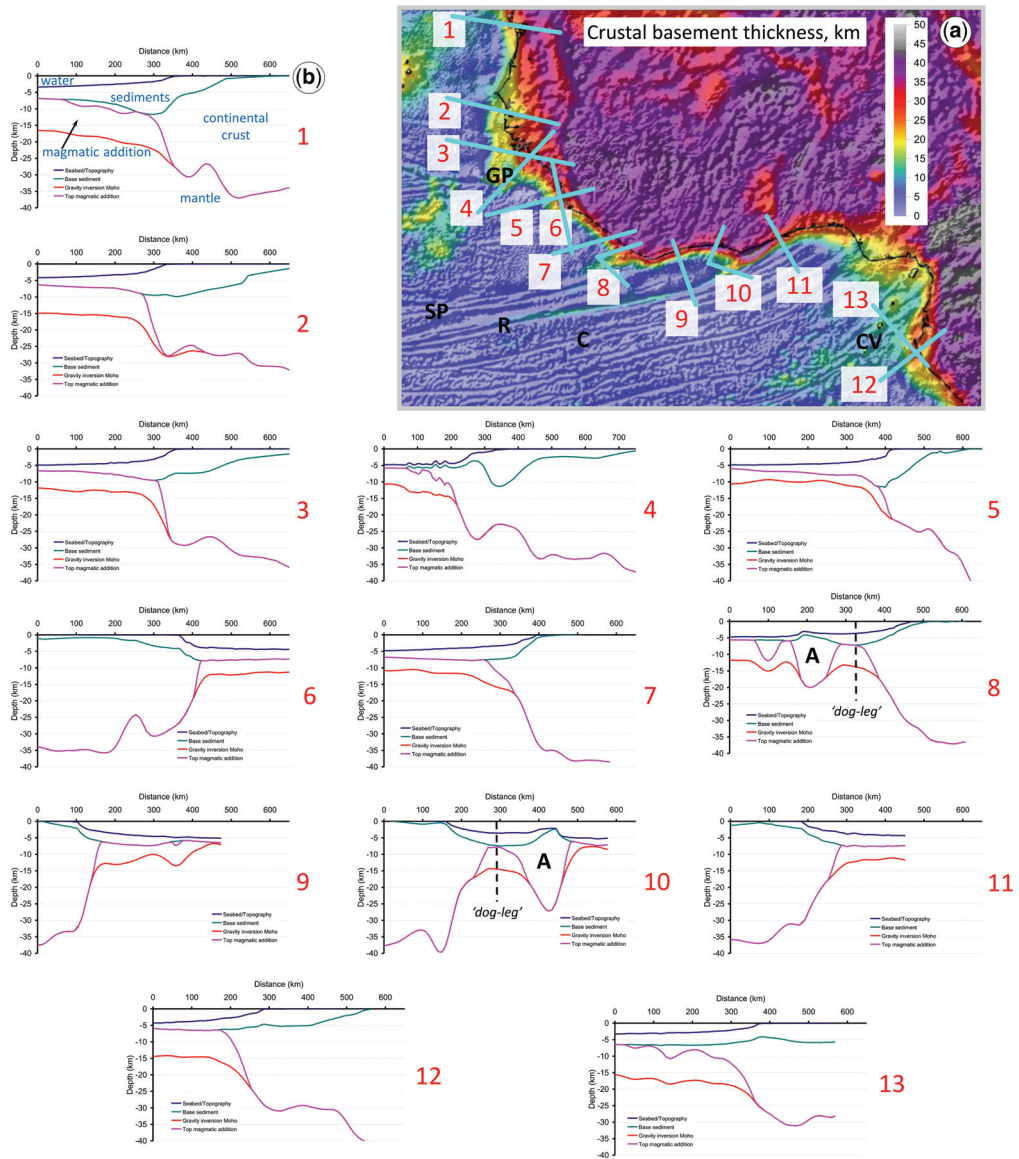
Fig. 8. (**a**) Map of total crustal basement thickness for the West African equatorial margin, enlarged from Figure 5a. Scale in kilometres. GP, Guinea Plateau; SP, St Paul's fracture zone; R, Romanche fracture zone; C, Chain fracture zone; CV, Cameroon volcanic line. The locations of the 13 cross-sections comprising (b) are shown. (**b**) Thirteen crustal-scale cross-sections extracted from the results of the gravity inversion. Sections 1–3 use a Jurassic break-up age of 170 Ma. Sections 4–13 use a Cretaceous break-up age of 110 Ma. Sections 3–11 determined assuming 'normal' magmatic addition. Sections 1, 2, 12 and 13 were determined assuming 'magma-rich' magmatic addition. Sections 1–3, 5, 7 and 12 cross rifted margin segments. Sections 4, 6, 9, 11 and 13 cross transform margin segments. Sections 8 and 10 are 'dog-leg' sections which cross both a rifted margin and an oceanic transform fault. On sections 8 and 10 A indicates areas of anomalously thick crust outboard of the COB (see text). (A higher-resolution display of the same cross-sections is available within Supplementary Material, Figure S1.)

extend on to oceanic crust which may not be related to the east–west Cretaceous opening of the Atlantic, but may instead be a fragment of oceanic crust

related to earlier Jurassic opening of the Central Atlantic and Gulf of Mexico (e.g. Pindell & Kennan 2009). Sections 1 and 2 have been produced with a

break-up age of 170 Ma (acknowledging Jurassic oceanic crust). Sections 3–15 have been produced with the standard Cretaceous break-up age for the Equatorial Atlantic of 110 Ma.

Ten of the 15 cross-sections have been produced from a gravity inversion model parameterized for 'normal' magmatic addition (Fig. 5c, e). The other five cross-sections (6, 9, 10, 11, 12) have been produced using decompression melting parameterized for 'magma-rich' magmatic addition (Fig. 5d, f).

With the exception of cross-section 15, all of the sections begin inboard on continental crust with no magmatic addition and end outboard on oceanic crust with no remaining continental crust. These 14 sections therefore all cross the OCT, either at a rifted margin or at a transform margin, depending on orientation. Cross-section 15 does not extend far enough south to reach predicted oceanic crust and in fact shows no magmatic addition because the trigger thinning factor of 0.7 (for normal decompression melting) has not been reached within the length of the section.

Five cross-sections have been produced using the parameterization for 'magma-rich' magmatic addition. The crustal thickness map (Fig. 7a) shows that all five sections (6, 9, 10, 11, 12) cross areas of crustal thickness at their outboard end which is thicker than the standard oceanic thickness of 7 km. For these lines the magmatic addition has therefore been increased to the magma-rich maximum of 10 km in order to test whether this will resolve thick oceanic crust (up to 10 km). This has worked for sections 6, 9 and 12. Caution should be used, however, in concluding that the break-up at these locations was necessarily magma-rich. Ocean drilling and deep-seismic-reflection data suggest that the oceanic crust in these regions experienced post-formation intra-plate magmatism of Late Cretaceous and Early Tertiary age, as observed on the Ceara Rise (Kumar & Embley 1977; Hekinian *et al.* 1978), which thickened what may have been normal (or even thin) oceanic crust.

On sections 10 and 11 even 'magma-rich' magmatic addition does not resolve continuous oceanic crust within the outboard domain and instead these two cross-sections show isolated crustal blocks greater than 10 km thickness (labelled A on the sections, Fig. 7b). These blocks almost certainly correspond to oceanic crust plus younger volcanic addition, resulting in magmatic thicknesses in excess of 10 km, rather than being isolated slivers of continental crust. This conclusion highlights that, wherever possible, regional geological knowledge should be used to assist interpretation of the gravity inversion results.

As with all predictive models, the reliability of the predictions is greater if the models can be independently validated. Figures 10–12 are used (below) to compare three of the South American cross-sections (3, 5, 6) with published cross-sections constructed from pre-existing data. Away from areas of validation, however, the power of extracting cross-sections from the gravity inversion models is that the sections provide an insight into rifted margin geometry in areas where this would not otherwise be possible. In this context such cross-sections may be used to help position long regional seismic lines across this particular margin, thus reducing uncertainty associated with an expensive commercial process.

Crustal structure of the West African equatorial margin

Figure 8 provides the equivalent display for the West African equatorial margin as that shown by Figure 7 for the South American margin. Figure 8a is a map of total crustal basement thickness, enlarged from Figures 3 and 5a. Figure 8b comprises 13 crustal-scale cross-sections extracted from the gravity inversion results.

The margin is again strikingly non-linear and partitioned into rift and transform segments by the same oceanic fracture zones which segment the South American margin, particularly so the very prominent St Paul's, Romanche and Chain fracture zones (Figs 3 & 8a). St Paul's and Romanche delineate longer transform-margin segments along the northern Gulf of Guinea than the width of the intervening rift segments. The 13 cross-sections have again been constructed so that they illustrate either rift segments within the current WSW–ENE opening direction, or transform segments orthogonal to this. Two of the sections (8 and 10) have right-angle bends in them so that they illustrate both rift and transform geometry, across the St Paul's and Romanche fracture zones respectively.

The northern three sections (1–3) lie north of the Cretaceous equatorial margin *sensu stricto* and extend on to Jurassic oceanic crust of the Central Atlantic and North Africa. These sections have therefore been produced with a break-up age of 170 Ma. Sections 4–13 have been produced with the standard Cretaceous break-up age for the Equatorial Atlantic of 110 Ma.

Nine of the 13 cross-sections have been produced from a gravity inversion model parameterized for 'normal' magmatic addition (Fig. 5c, e). The other four cross-sections (1, 2, 12 and 13) have been produced from a model parameterized for 'magma-rich' magmatic addition (Fig. 5d, f). All of the sections begin inboard on continental crust with no magmatic addition and end outboard on oceanic crust with no remaining continental crust. They therefore all

cross the OCT, either at a rifted margin or at a transform margin, depending on orientation.

Some explanation of the 'magma-rich' sections is again required. The crustal thickness map (Fig. 8a) shows that all four sections (1, 2, 12, 13) extend outboard on to areas of crust which are thicker than the standard oceanic thickness of 7 km (c. 10 km thick). In these areas the magmatic addition within the gravity inversion has therefore been increased to the magma-rich maximum of 10 km in order to see if this will resolve thick oceanic crust (up to 10 km). This works for all four sections, producing oceanic crust thicker than 7 km at the outboard end of each section. For sections 1 and 2 (Jurassic oceanic crust) this result is not a surprise as the conjugate North American Jurassic margin is commonly considered to be a 'magma-rich' margin (Eldholm et al. 2000). Further south, section 13 crosses the Cameroon volcanic line (post-break-up seamounts), while section 12 lies close to it. Thus, while magmatic crust thicker than 7 km on these two sections may have been produced during break-up, it could also have been enhanced in thickness by the more recent post-break-up Cameroon Line volcanics (Gallacher & Bastow 2012).

Within the 13 West African sections the most complex crustal geometries are seen on sections 8 and 10, which are the two 'dog-leg' sections crossing major transform faults. On both sections the inboard c. 300 km crosses a rifted margin segment, with the continental crust thinning from c. 35 km to 0, at which point it is replaced by 7 km of oceanic crust. For the next (outboard) c. 300 km both sections dogleg to the south, crossing the St Paul's and Romanche fracture zones, respectively. As the fracture zones are crossed the crustal basement thickens again to c. 15 km on section 8 and c. 20 km on section 10 (labelled A on the sections). On the South American margin, blocks of anomalously thick crust close to fracture zones (Fig. 7, sections 10 and 11) were interpreted as oceanic crust thickened by post-break-up magmatism. Along the St Paul's and Romanche fracture zones, however, there is no indication of post-break-up magmatism (it is encountered further to the south along the Cameroon volcanic line; Fig. 8). We therefore believe that other possible explanations are required for the presence of the thick crust adjacent to and immediately north of the two major fracture zones on the African side. These possibilities include:

(1) they are blocks of continental crust which have been extended oceanwards along the fracture zones during the break-up process;
(2) they are areas of oceanic crust magmatically thickened along the fracture zones by the early post-break-up passage of the spreading centre to the south;

(3) they are areas of oceanic crust tectonically thickened by mild transpression (during the passage of the spreading centre) along the inside arc of the curved fracture zones.

The gravity inversion alone cannot distinguish between these three possibilities, but given the prediction of oceanic crust on both cross-sections 8 and 10 north of the fracture zones (where the 'dog-leg' bends are located; Fig. 8), we consider option 1 the least likely and favour a magmatic composition for the areas of thick crust. These possibilities are discussed again later in the paper.

West African section 4 also shows a crustal geometry which is more complex than a 'simple' progressive thinning of continent into ocean. An enlargement of this cross-section, together with the associated profile of thinning factor $(1 - 1/\beta$; Fig. 5e) is shown in Figure 9. The section has its inboard (NE) end located c. 200 km onshore and across a distance of c. 400 km the continental basement thins steadily from c. 36 to c. 12 km, at which point the thinning factor has reached c. 0.7. Over the next 100 km, however, the continental basement thickens again to c. 24 km (thinning factor <0.4), before finally thinning once more, this time to zero (thinning factor 1) and being replaced by oceanic crust. There is thus an anomalously thick crustal block towards the outboard end of the section, which corresponds to the bathymetric feature known as the Guinea Plateau (Figs 3, 8 & 9). In this particular case we believe that the crustal block is indeed likely to be continental crust and we interpret the area of thin crust (c. 12 km) immediately inboard to be a 'failed break-up basin' (FBB on Fig. 9, e.g. Scotchman et al. 2010; Fletcher et al. 2013). Failed break-up basins occur at continental margins as rift basins which were the locus of an initial attempt at break-up, but which were subsequently abandoned as final break-up occurred further outboard. This is probably the consequence of two en echelon rift segments propagating towards each other but failing to connect directly (Scotchman et al. 2010, fig. 8; Fletcher et al. 2013, figs 12 & 13). Section 4 lies at the boundary between Jurassic Central Atlantic oceanic crust to the north and Cretaceous Equatorial Atlantic oceanic crust to the south. It is quite likely that the 'failed break-up basin' in this location results from the attempt (ultimately successful) to link the developing Cretaceous margin into the pre-existing Jurassic margin. If the Jurassic margin and the propagating Cretaceous margin were initially laterally offset from each other, the crustal configuration following final break-up could have been a failed break-up basin at the northern end of the initial Cretaceous rift. The pre-break-up conjugacy of the Guinea Plateau and 'failed break-up basin' (Fig. 9) with the Demerara Plateau on the South American margin
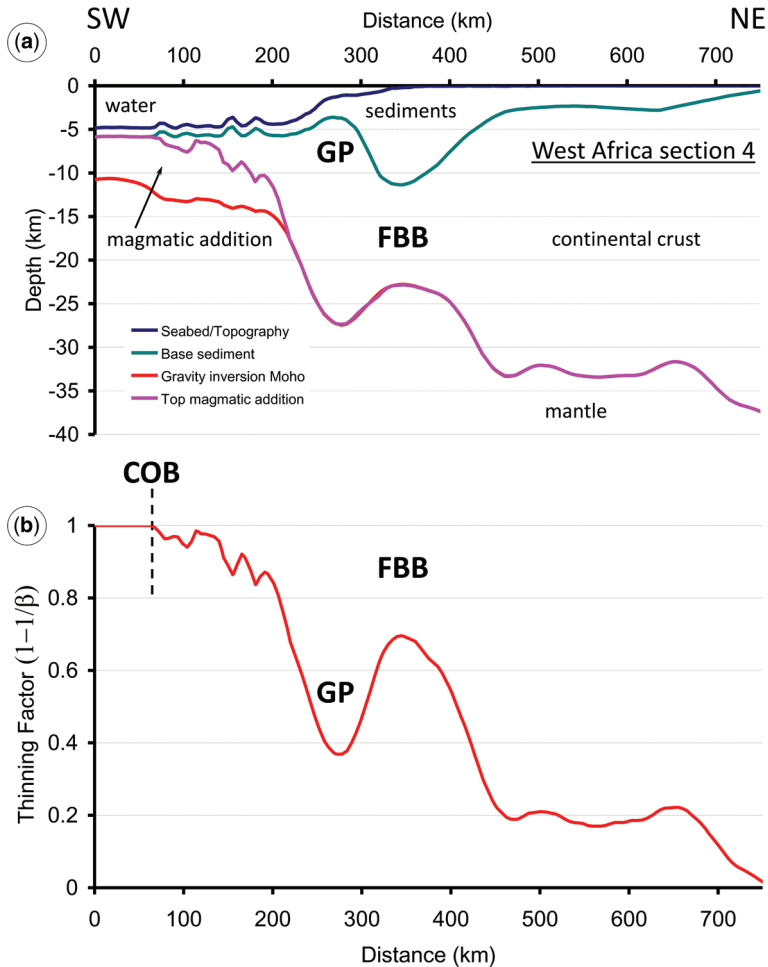
Fig. 9. (**a**) Enlargement of West African section 4, see Figure 8a for location. FBB indicates the location of thin continental crust and a possible 'failed break-up basin' inboard of the COB. GP indicates the location of thick continental crust below the Guinea Plateau, between the COB and the FBB. (**b**) Profile of thinning factor for section 4. Thinning factor rises to *c.* 0.7 within the 'failed break-up basin', before dropping to 0.4 to the west at the Guinea Plateau where the continental crust thickens once more. Thinning factor reaches 1 in the oceanic area at the western end of the section.

(Fig. 3) is illustrated later in the context of the plate reconstructions.

Validation of the cross-sections by comparison with pre-existing data

The power of the crustal cross-sections derived from gravity inversion is that they can be used to make predictions about crustal type and crustal structure for areas in which there has been no local acquisition of seismic data. As with all models, if the results can in some way be validated by comparison with pre-existing information then confidence in their

predictions is increased. Figures 10–14 show five of the cross-sections produced by gravity inversion compared with five previously published cross-sections, three on the South American margin (Figs 10–12) and two on the West African margin (Figs 13 & 14).

South American section 3

Figure 10a shows an enlargement of South American cross-section 3 (Fig. 7), together with a crustal cross-section from nearby to the east constructed by Green-royd *et al.* (2008) from wide-angle and reflection seismic data plus supporting gravity modelling
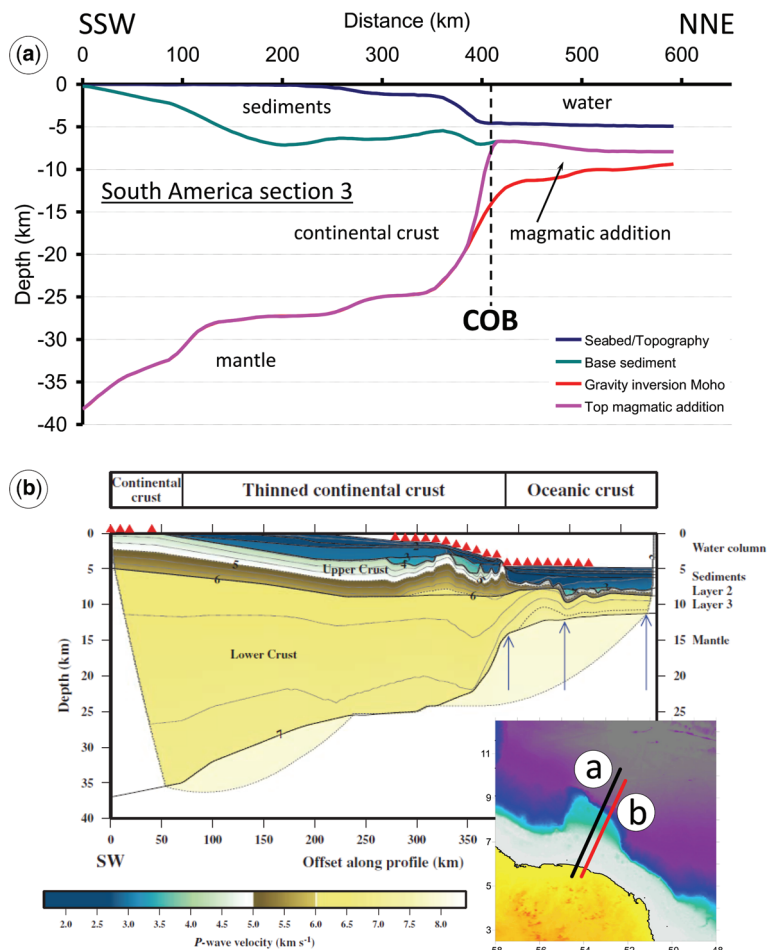
Fig. 10. Validation of South American section 3 determined using OCTek gravity inversion. (**a**) Enlargement of South American section 3, see Figure 7a for location. (**b**) Crustal cross-section produced from wide-angle and reflection seismic data by Greenroyd *et al.* (2008) (see inset map for location). The similarity in illustrated crustal geometries and crustal types is striking and thus (b) provides a good validation of the predictions from gravity inversion.

(Fig. 10b). The sections strike slightly east of north, crossing the Demerara Plateau (offshore Suriname and French Guyana) and its northern margin with the Atlantic (Fig. 7a). This margin is interpreted by both ourselves and Greenroyd *et al.* to be a Cretaceous transform margin. In the regional crustal-thickness map (Fig. 3) the northern margin of the Demerara Plateau is clearly bounded by a major oceanic fracture zone extending across the full width of the Equatorial Atlantic from South America to West Africa.

The crustal geometries and the crustal types picked out by both sections are very similar. Both sections show the same 'gentle' tapering of the continental crust northwards towards the transform

margin. The transform margin then shows a very abrupt step from continental crust (*c.* 15 km thick) on to relatively thin oceanic crust (*c.* 5 km thick). The Greenroyd *et al.* section, derived primarily from acquired seismic data, provides a very good validation of the likely accuracy of the nearby cross-section from the regional gravity inversion.

South American section 5

Figure 11a shows an enlargement of South American cross-section 5 (Fig. 7), together with an intersecting but clockwise-oblique crustal cross-section constructed by Greenroyd *et al.* (2007) from wide-angle and reflection seismic data (Fig. 11b). The sections
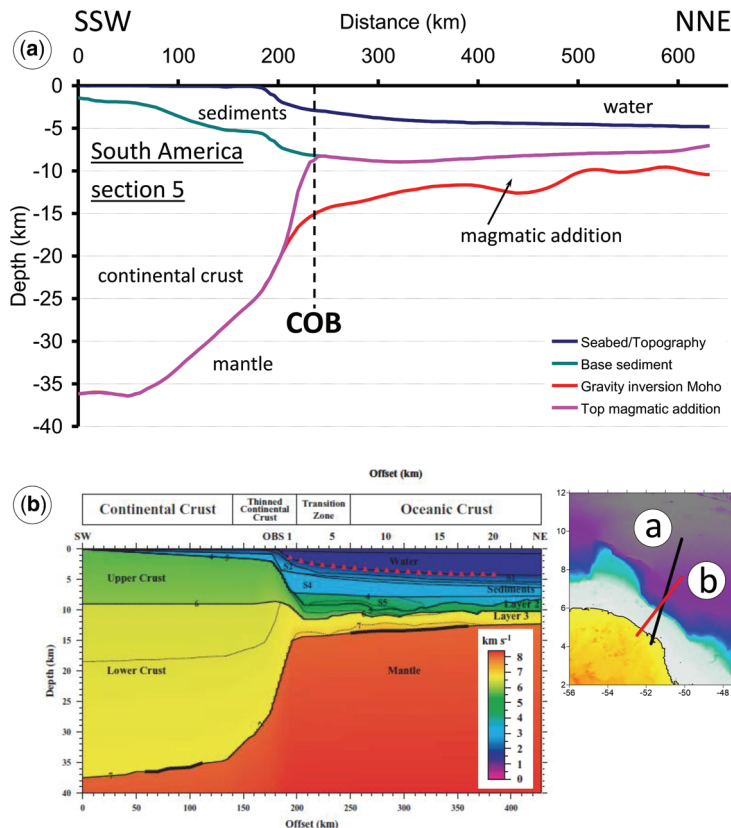
Fig. 11. Validation of South American section 5 determined using OCTek gravity inversion. (**a**) Enlargement of South American section 5, see Figure 7a for location. (**b**) Crustal cross-section produced from wide-angle and reflection seismic data by Greenroyd *et al.* (2007) (see inset map for location). The similarity in illustrated crustal geometries and crustal types is striking and thus (b) provides a good validation of the predictions made from gravity inversion.

both strike slightly east of north (offshore French Guyana) and are broadly parallel to section 3 (Fig. 10, *c.* 300 km to the west). Section 5 does not cross the offshore Demerara Plateau but rather passes relatively rapidly (<200 km) from onshore continent on to Cretaceous oceanic crust. Both sections show a sharp continental margin and abrupt thinning of continental crust which is replaced to the north by relatively thin (*c.* 5 km) oceanic crust.

Greenroyd *et al.* (2007) describe the line location as a 'rift-type setting', which may simply refer to the presence of an attenuated continental margin, but we believe that in detail the two sections quite clearly cross another sharp transform margin, delineated by a clear oceanic fracture zone at the COB (Figs 3 & 7).

Regardless of any potential kinematic interpretation, the similarities between crustal geometry and crustal type on both sections provide another very good validation of the predictive cross-section from the regional gravity inversion.

South American section 6

Figure 12a shows an enlargement of South American cross-section 6 (Fig. 7), together with a crustal cross-section from a nearby location (but with a different orientation) constructed by Watts *et al.* (2009) from wide-angle and reflection seismic data (Fig. 12b). Section 6 extends eastwards from the coast of French Guyana (Fig. 7a) and crosses what we interpret to be a rifted continental margin, with the section lying along the direction of oceanic spreading. At its eastern end, on oceanic crust, section 6 intersects the Watts *et al.* section, which itself extends SW from here on to the Brazilian coast, at *c.* 45° to section 6 (see inset map in Fig. 12b).
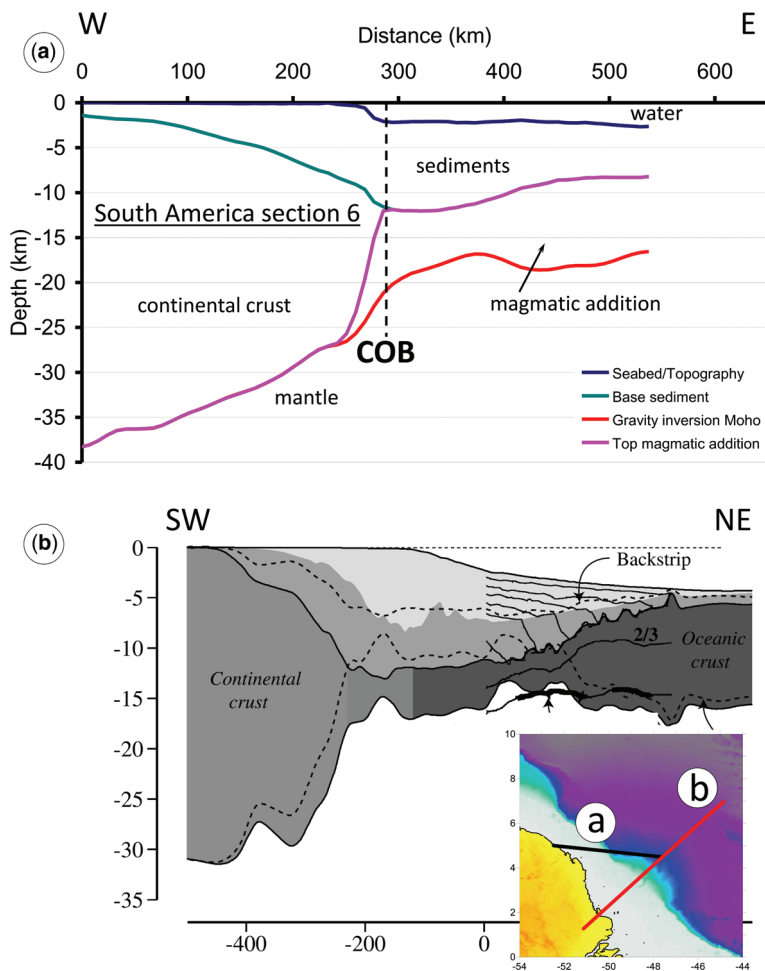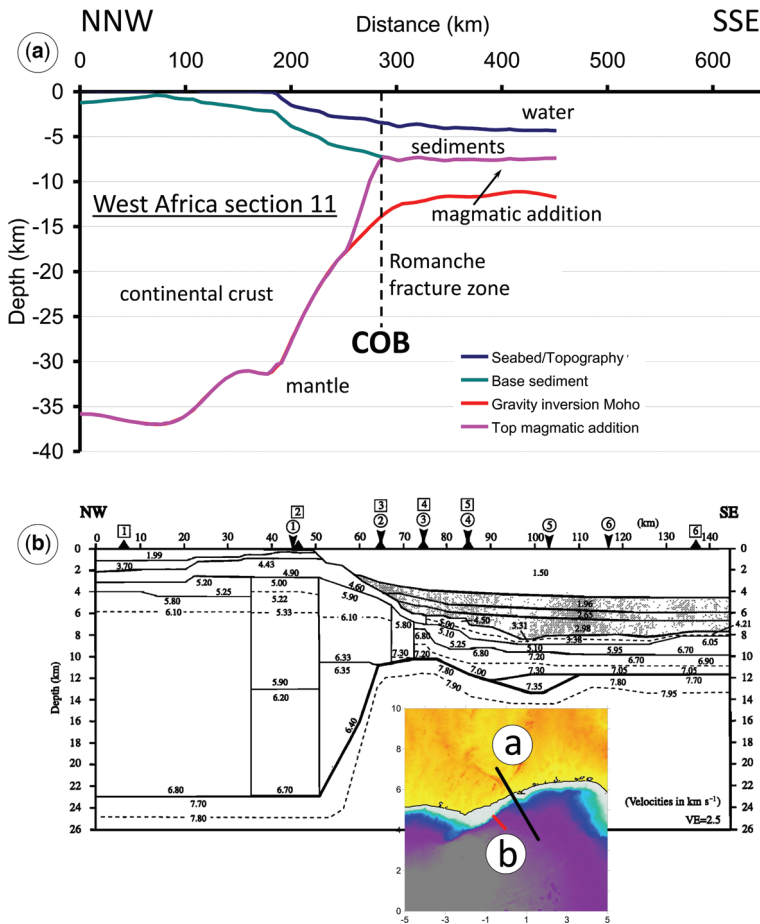
Fig. 12. Validation of South American section 6 determined using OCTek gravity inversion. (**a**) Enlargement of South American section 6, see Figure 7a for location. (**b**) Crustal cross-section orientated at *c.* 45° to (a) but intersecting it at its outboard, eastern oceanic end (see inset map for location). The section was produced from wide-angle and reflection seismic data by Watts *et al.* (2009). The similarity in illustrated crustal geometries and crustal types is striking and thus (b) provides a good validation of the predictions made from gravity inversion.

Despite their geographical divergence away from the oceanic intersection, the two cross-sections show very similar crustal geometries and predicted crustal types, providing further corroboration of the results from the gravity inversion. Both sections begin in the west on thick continental crust, which thins across *c.* 250 km (the rifted margin) into a layer of very thin crust (<5 km thick). Both our gravity inversion and the seismic study of Watts *et al.* interpret this thin crust to be thin oceanic crust (thinning factor 1 in the gravity inversion). The geometry of this thin crust is similar to that reported by Funck *et al.* (2003) and Hopper *et al.* (2007) for the SCREECH 1 line on the NE Newfoundland margin, which is a magma-poor margin on which mantle exhumation has been

identified. Outboard of the thin crust, the crustal basement thickens to normal, or slightly greater than normal, oceanic values (Figs 3 & 7). Both ourselves and Watts *et al.* interpret this to be thicker oceanic crust, younger than the break-up event. In order to resolve this area of thick crust as oceanic (rather than thinned continental), the gravity inversion must be parameterized for magma-rich magmatic addition (see discussion above and Fig. 5).

The successful comparison and validation presented here for three cross-sections in the area of Suriname, French Guyana and northernmost Brazil gives some confidence in the interpretation of results from the gravity inversion and associated cross-sections further to the south along the South

Fig. 13. Partial validation of West African section 11 determined using OCTek gravity inversion. (**a**) Enlargement of West African section 11, see Figure 8a for location. (**b**) Crustal cross-section produced from wide-angle seismic data by Edwards *et al.* (1997) (see inset map for location). The crustal geometries and crustal types illustrated in both sections are similar, but the continental Moho is predicted to be deeper on (a) from gravity inversion (*c.* 35 km) than it is on (b) from seismic (*c.* 23 km). The validation is therefore not complete, but the seismic Moho in (b) at *c.* 23 km does seem surprisingly shallow for onshore Africa.

American equatorial margin, in areas where there are no published cross-sections available for comparative purposes.

West African section 11

Figure 13a shows an enlargement of West African cross-section 11 (Fig. 8), together with a (shorter) crustal cross-section from further to the SW along the same margin segment, constructed by Edwards *et al.* (1997) from wide-angle seismic data (Fig. 13b). Both sections cross the transform margin delineated by the Romanche fracture zone, where it lies close to the coastline of Ghana. This is thus a COB in both geological and geographical terms.

Both sections illustrate the sharpness of the COB across the fracture zone, thick continental crust to the north being replaced by oceanic crust to the south across a few tens of kilometres. The continental Moho of Edwards *et al.* is, however, surprisingly shallow, essentially flat at 23 km. This is difficult to explain in the light of the regional gravity inversion (and also isostatic arguments), which consistently places the West African Moho at 35 km or deeper (Fig. 5a).

There is better agreement in crustal thickness south of the fracture zone where both sections show the oceanic crust to be relatively thin (*c.* 5 km). We have also made this observation about the oldest oceanic crust on the three validated South American
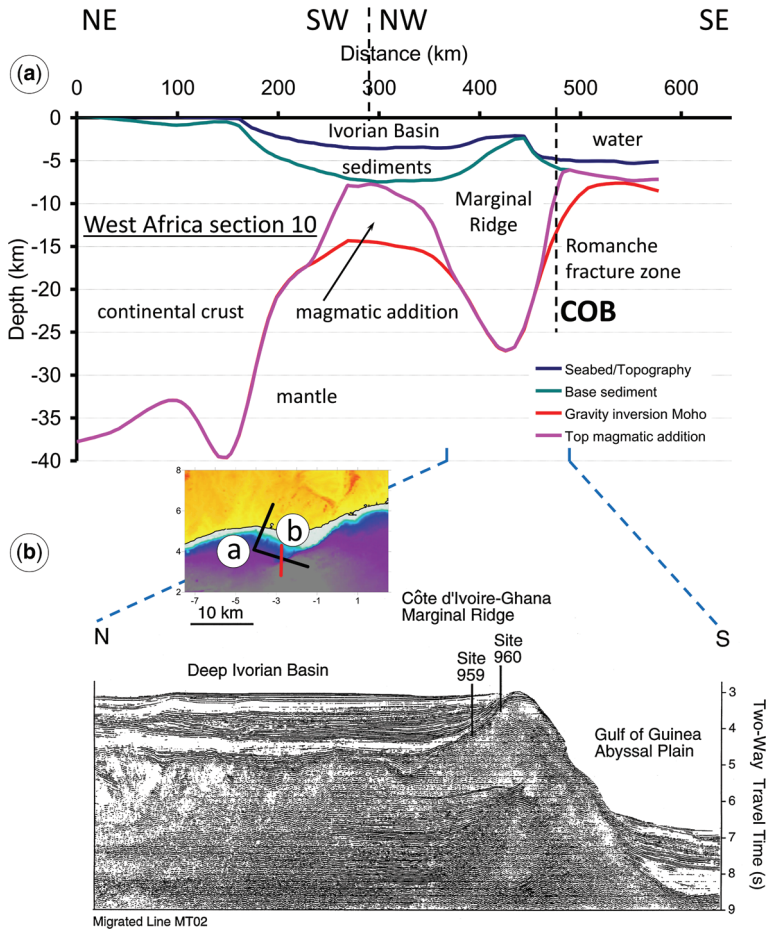
Fig. 14. (**a**) Enlargement of West African (dog-leg) section 10 determined using OCTek gravity inversion, see Figure 8a for location. (**b**) Seismic section from Clift *et al.* (1997), *c.* 100 km in length, crossing the Romanche fracture zone at an angle to section 10 (see inset map for location). The prominent Marginal Ridge immediately north of the Romanche fracture zone is clear on both sections. (a) shows the Marginal Ridge to be underlain by thick crust, *c.* 20 km. While this could be a continental block (Clift *et al.*), it could also a be block of thickened magmatic crust (see text).

profiles (Figs 10–12), a result which possibly indicates slow spreading on both margins of the early Equatorial Atlantic.

The crustal geometries and crustal types on the two sections match well, but the thickness of the continental crust in the two models is different. We therefore have a partial, but not complete, comparison and validation of the gravity inversion results. We suggest that, in the light of the regional gravity inversion results, the continental Moho depth from the wide-angle experiment could be re-examined.

West African section 10

Figure 14a shows an enlargement of West African cross-section 10 (Fig. 8), together with a seismic line (from Clift *et al.* 1997; also Basile *et al.* 1993; Sage *et al.* 2000) which intersects the southern part of section 10 (Fig. 14b). Both cross the Romanche fracture zone, offshore Côte d'Ivoire. In detail the seismic line strikes clockwise of section 10 (Fig. 14 inset map) and is considerably shorter (*c.* 100 km in length). North of the Romanche fracture zone the seismic line lies NE of section 10 and further inboard with respect to the continental margin. With no wide-angle seismic data available this is not a validation of the Moho and crustal-thickness predictions of the gravity inversion, but rather an illustration of the crustal geometries across the Romanche fracture zone resolved by the gravity inversion.

The central focus of the seismic line is the 'Marginal Ridge', along and to the immediate north of the

Romanche fracture zone. Both Clift *et al.* (1997) and Sage *et al.* (2000) considered the Marginal Ridge, at the location imaged by the seismic line, to be underlain by continental crust and thus part of the continental margin, which is anomalously thick along the fracture zone. Clift *et al.* (fig. 1) also showed that to the north of the Marginal Ridge the seismic line is interpreted to lie inboard (to the east) of the COB, which bounds the rifted margin of the Deep Ivorian Basin. Section 10 extends NW to a more distal location north of the Romanche fracture zone (Fig. 14 inset map) and makes predictions of possibly different crustal-types in this area.

The Ivorian Basin on section 10 (Fig. 14a) is predicted by the gravity inversion (parameterized for normal magmatic addition) to be underlain by magmatic crust, which in the centre of the basin has completely replaced the continental crust, making this an oceanic setting. Section 10 is therefore interpreted to lie outboard of the COB within the Ivorian Basin. The crustal affinity of the Marginal Ridge on section 10 (which is where it intersects the seismic line) is less definitive. The gravity inversion resolves a crustal block *c.* 20 km thick, which by default is identified as continental as it is too thick even for a parameterization with magma-rich magmatic addition. As outlined above, in discussion of West African sections 8 and 10 (Fig. 8), we believe there are three possible explanations for the presence of thick crust on the Marginal Ridge:

(1) continental crust extended along the fracture zone (the interpretation of Clift *et al.* 1997);
(2) oceanic crust magmatically thickened by the passage of the spreading centre;
(3) oceanic crust thickened by mild transpression along the fracture zone.

The latter two possibilities were recognized by Clift *et al.* as potential contributors to the geometry of the Marginal Ridge, although they favoured option 1. The gravity inversion alone cannot distinguish between these three possibilities on section 10, but given the prediction of oceanic crust within the Ivorian Basin north of the fracture zone we would favour a magmatic affinity for the Marginal Ridge at the location of section 10. It is notable that the Romanche, St Paul and Chain fracture zones all show a significant anti-clockwise change in their orientation to the NE, close to the African coast (Figs 3 & 8a). This indicates that a change in the divergence vector occurred between Africa and South America during early seafloor spreading, while the spreading centre migrated west along the fracture zones, providing a possible mechanism for transpressional thickening of pre-existing oceanic crust along the inside arc of the fracture zones (option 3 above).

In a recent paper Nemčok *et al.* (2016) have suggested that the Marginal Ridge (their Ghana Ridge) is a detached microcontinental fragment which has been translated 133 km WSW along the Romanche fracture zone. They equate it to two other microcontinental blocks which have been dredged further west along the fracture zone. We believe that it is unlikely that the Marginal Ridge is an allochthonous block because neither our maps (Figs 3 & 8a) nor the maps of Nemčok *et al.* (figs 1 & 2) show a continuous fracture zone or major fault along the northern margin of the Marginal Ridge. Such a fault is required in order to accommodate the 133 km displacement.

Finally, while there is no validation or comparison data available for the sections we have produced in the northern part of equatorial West Africa, three of which extend on to Jurassic oceanic crust (sections 1–3, Fig. 8), we would draw attention to the results of the DAKHLA wide-angle seismic experiment (Klingelhoefer *et al.* 2009) north of our AOI, offshore Western Sahara. The DAKHLA experiment provides crustal profiles extending on to the Central Atlantic Jurassic oceanic crust and shows a similar crustal structure in the OCT to that determined by OCTek gravity anomaly inversion in this area.

Equatorial Atlantic plate reconstructions

In the discussion so far we have attempted to show how gravity inversion of publicly available datasets can be used to provide information about 3D crustal geometries along deep-water continental margins. In this final discussion we will attempt to show how the results of the gravity inversion are not only relevant to our understanding of present-day margin structure but can also be used as input to quantitative models of margin history by constraining plate reconstructions.

Plate reconstructions commonly use ephemeral geomorphic features such as present-day bathymetry and coastlines to constrain the final 'closed' geometry of a restoration sequence. At the time of break-up neither the present-day coast nor shelf-breaks existed and so the restorations could potentially be better constrained by using geological features present at this time in the past.

Figure 15 shows a sequential plate reconstruction of the area covered by the crustal-thickness map in Figure 3. This focuses on the Equatorial Atlantic but also extends north into the Central Atlantic and south into the South Atlantic. The restorations have been performed in GPlates 1.5 (http://www.gplates.org), which is publicly available software. The geological property being restored by the restorations is total crustal basement thickness, which is the product of both the break-up process and subsequent seafloor spreading. Total crustal thickness

Restored crustal basement thickness, km
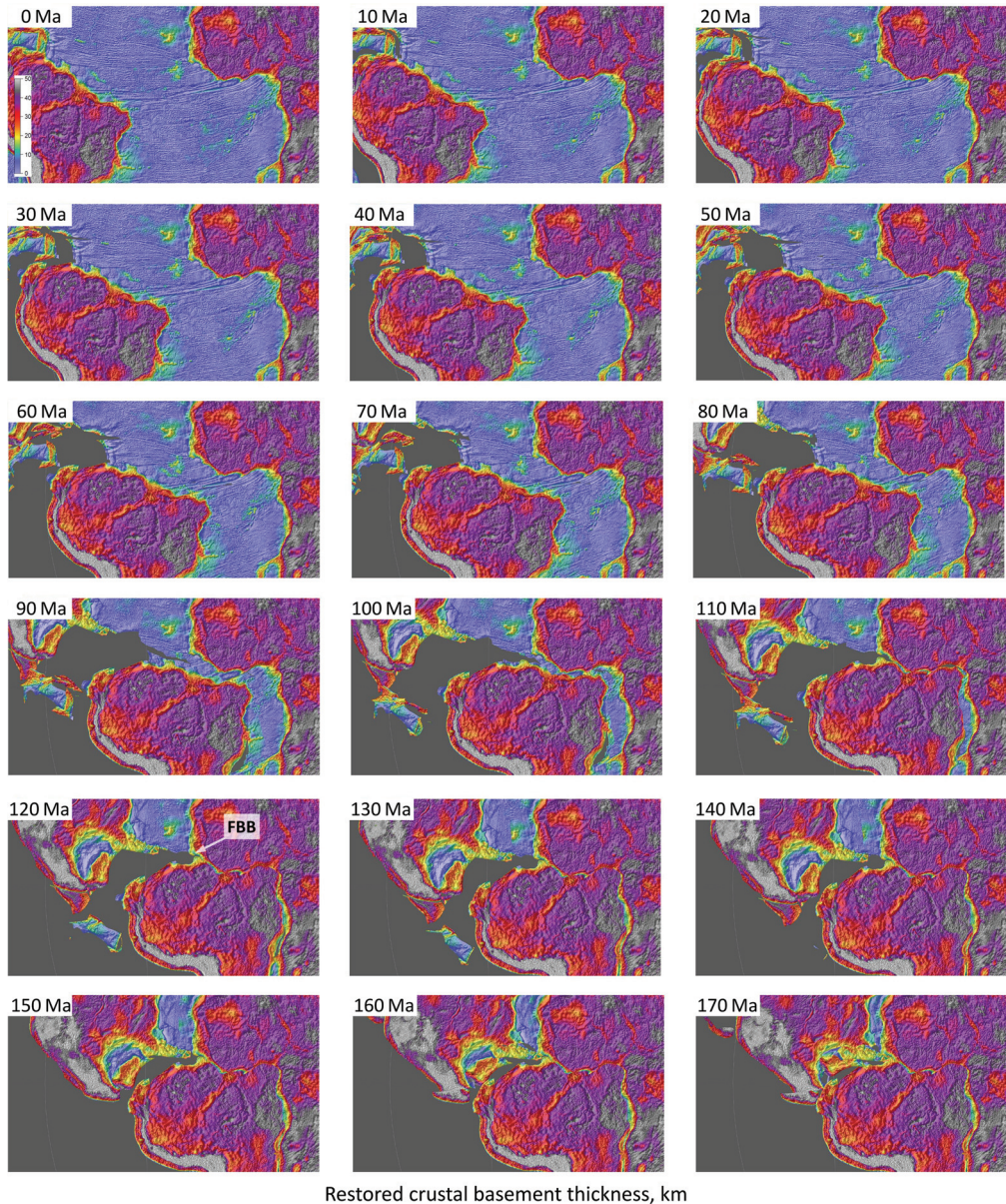
Fig. 15. Plate reconstruction, using GPlates 1.5, of the Central-Equatorial–South Atlantic. The plate reconstructions are populated with the map of total crustal basement thickness (continental and oceanic) from gravity inversion (Fig. 3). The reconstruction is illustrated at increments of 10 Ma, back to 170 Ma. First oceanic crust in the Equatorial Atlantic forms between 110 and 100 Ma. Use of the crustal thickness map allows long-term geological features to be restored, rather than the more typical use of present-day bathymetric features and coastlines. FBB on the restoration at 120 Ma indicates the location of a possible 'failed break-up basin' lying east of the restored and now adjacent Guinea Plateau and Demerara Plateau (see also Figs 3, 8 & 9). (A higher-resolution display of the same plate reconstructions is available within Supplementary Material, Figure S2a.)

does not distinguish crustal type (continental or oceanic), but Figure 16 shows the same set of restorations restoring the corresponding map of thinning factor (Fig. 5), which accounts for predicted magmatic addition and in which oceanic areas are defined by thinning factor = 1 (coloured white).

Restored continental-lithosphere thinning-factor
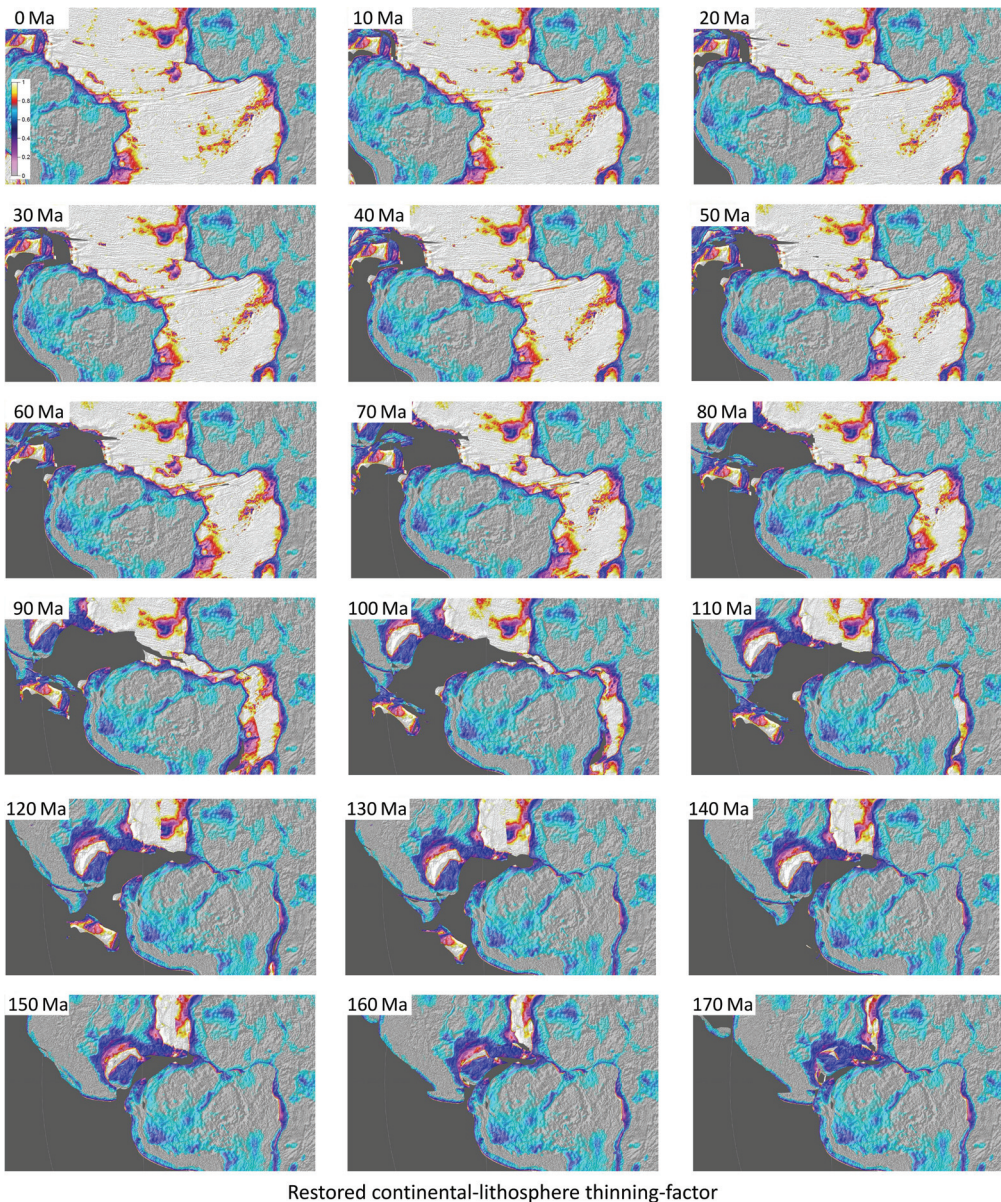
Fig. 16. The same plate restoration sequence as in Figure 15 but with the plate reconstructions populated with the map of thinning factor from gravity inversion (Fig. 5). Use of thinning factor allows oceanic areas to be identified as white (thinning factor 1) in each stage of the reconstruction. (A higher-resolution display of the same plate reconstructions is available within Supplementary Material, Figure S2b.)

The plate reconstructions (Figs 15 & 16) are shown at time increments of 10 Ma and use the default GPlates 1.5 rotation poles, plate polygons and ocean isochrons to constrain plate motions (Seton *et al.* 2012). The restorations extend from the present day back to 170 Ma, thus, not only do they illustrate restoration of the (Cretaceous)

Equatorial Atlantic, but they also illustrate restoration of the older (Jurassic) Central Atlantic. Rather than describe each step of the restoration, we will simply highlight the key points of the full sequence.

Prior to 110 Ma restorations show that the Equatorial Atlantic was closed. Continental break-up for the Equatorial Atlantic, defined as the generation of

the first oceanic crust, occurred between 110 and 100 Ma. By 100 Ma a series of discrete, isolated oceanic basins with a trapezoidal geometry had formed but did not form a through-going, deep-water, ocean–basin system. These trapezoidal basins were bounded north and south by transform faults and east and west by oblique rifted continental margins. The continental crust of South America and Africa was still connected in some places at this time. By 90 Ma, Africa and South America were separated by oceanic crust and we expect there to have been deep-water oceanic connectivity of the Equatorial Atlantic with both the Central and South Atlantic.

The restorations from 170 to 110 Ma show the development of the opening of the Central Atlantic prior to the opening of the Equatorial Atlantic. They show the plate-tectonic context of the development of the South American margin to the west of the Demerara Plateau (Fig. 3) and its relationship to the formation of the Central Atlantic and Gulf of Mexico.

To the south, the plate restorations show that, while the southern South Atlantic started to open at 130 Ma, significant oceanic connectivity of the Equatorial Atlantic to the south did not occur until Albian times (110 Ma or younger). The restorations to 110 Ma and older show the relationship of the (onshore) South American and West African basins formed prior to Equatorial Atlantic break-up.

The restoration at 120 Ma allows us to add more insight into the 'failed break-up basin' inboard of the Guinea Plateau on the West African margin (Figs 3 & 9). This restoration shows that the 'failed break-up basin' inboard of the Guinea Plateau was initially directly along strike to the north of (and linked to) the rifted margin defining the eastern flank of the Demerara Plateau on the conjugate South American margin. The Guinea Plateau and the Demerara Plateau probably began to extend together at c. 120 Ma or earlier, prior to break-up. By 110 Ma the eastern flank of the Demerara Plateau had successfully separated from West Africa, but the 'failed-break-up basin' and the Guinea Plateau remained attached to West Africa as the final break-up transferred displacement along the northern flank of the Demerara Plateau and propagated northwards along the western flank of the Guinea High (Figs 9 & 15).

The plate reconstructions in Figures 15 and 16 are not new in the sense of providing new kinematic information about plate motions across the Atlantic; they use the prior information about plate motions contained within GPlates. What is new, however, is that the restorations are the first to incorporate a full crustal model (continental and oceanic) within the properties of the restored plates and thus illustrate the restored plates in a new and informative way. As with most of the work presented in this paper, we have focused on the plate restorations at a very large scale, but at a more focused scale across the Equatorial Atlantic the same restorations have been used to help to constrain palaeogeographical models for exploration scoping studies.

Concluding summary

The principal objective of this paper has been to show how regional-scale gravity inversion can be used to provide a 3D crustal model of rifted margin geometry, in circumstances where little or no other data (particularly seismic data) may be available. The technique provides important geological information about any area to which it is applied, but its particular strength lies in application to petroleum exploration scoping studies, where it provides a cost-effective entry point into basin analysis.

In other papers (e.g. Roberts *et al.* 2013; Cowie *et al.* 2015, 2016) it has been shown how the gravity inversion technique can be used as one of a suite of tools for deep-water basin analysis. Such additional tools might include subsidence analysis and analysis of residual-depth-anomalies, both of which require supporting seismic-reflection data. Our purpose in this paper, however, has been to demonstrate the use of the gravity inversion technique on its own. The gravity inversion technique therefore provides a good starting point in a frontier exploration setting where little or no seismic reflection data is available.

The primary output from the gravity inversion is a suite of maps which show:

- Moho depth;
- total crustal basement thickness (continental or oceanic);
- residual thickness of the continental crust;
- continental lithosphere stretching factor (β) and thinning factor (γ), where $\gamma = 1 - 1/\beta$.

These maps capture a 3D crustal model for continental areas, oceanic areas and the rifted margins in between. Our understanding of the results is helped by extracting crustal cross-sections. The cross-sections themselves are a powerful predictive tool, but may themselves be compared with and validated against other data, such as wide-angle and reflection seismic data. Conversely the results of the gravity inversion can be used to validate or constrain interpretation of deep-seismic reflection data, by providing realistic bounds for crustal thickness and Moho position.

In our investigation of the Equatorial Atlantic, maps of crustal-thickness and conjugate-margin stretching have been used to illustrate how the Equatorial Atlantic opened as a set of stepped rift-transform segments, rather than as a simple orthogonal rifted margin. This has resulted in complex crustal geometries within the basins along the

margins, which have been illustrated with a series of cross-sections. On both margins anomalously thick crust is resolved along a number of oceanic fracture zones and we have discussed the possible origins for this. The cross-sections also show that while 'normal thickness' oceanic crust (*c.* 7 km) predominates in the equatorial region, areas of thinner (*c.* 5 km) and thicker (*c.* 10 km) oceanic crust are also present on both margins.

By using the results of the gravity inversion as input to plate reconstructions, the regional palaeo-geography of the Equatorial Atlantic during and after break-up has been displayed, in the context of the diachronous opening of the Central and South Atlantic on either side.

Although not covered specifically in this paper, the results of the gravity inversion can also be used as the input for further analysis. In particular, by quantifying (1) the thickness of the continental crust and (2) the magnitude of lithosphere stretching, two of the main uncertainties for the prediction of basement heat-flow are addressed and maps of top basement heat flow can be produced which draw directly on the results of the gravity inversion (e.g. Cowie & Kusznir 2012*a*).

References

ALVEY, A. 2010. *Using crustal thickness and continental lithosphere thinning factors from gravity inversion to refine plate reconstruction models for the Arctic & North Atlantic*. PhD thesis, University of Liverpool.

ALVEY, A., GAINA, C., KUSZNIR, N.J. & TORSVIK, T.H. 2008. Integrated crustal thickness mapping and plate reconstructions for the high Arctic. *Earth and Planetary Science Letters*, **274**, 310–321, https://doi.org/10.1016/j.epsl.2008.07.036

BASILE, C., MASCLE, J., POPOFF, M., BOUILLIN, J.-P. & MASCLE, G. 1993. The Côte d'Ivoire–Ghana transform margin: a marginal ridge structure deduced from seismic data. *Tectonophysics*, **222**, 1–19.

CHAPPELL, A.R. & KUSZNIR, N.J. 2008. Three-dimensional gravity inversion for Moho depth at rifted continental margins incorporating a lithosphere thermal gravity anomaly correction. *Geophysical Journal International*, **174**, 1–13.

CLIFT, P.D., LORENZO, J., CARTER, A., HURFORD, A.J. & ODP 159 SCIENTIFIC PARTY 1997. Transform tectonics and thermal rejuvenation on the Côte d'Ivoire–Ghana margin, west Africa. *Journal of the Geological Society, London*, **154**, 483–489, https://doi.org/10.1144/gsjgs.154.3.0483

COWIE, L. & KUSZNIR, N.J. 2012*a*. Gravity inversion mapping of crustal thickness and lithosphere thinning for the eastern Mediterranean. *The Leading Edge*, **July 2012**, 810–814.

COWIE, L. & KUSZNIR, N.J. 2012*b*. Mapping crustal thickness and oceanic lithosphere distribution in the Eastern Mediterranean using gravity inversion. *Petroleum Geoscience*, **18**, 373–380, https://doi.org/10.1144/petgeo2011-071

COWIE, L., KUSZNIR, N.J. & MANATSCHAL, G. 2015. Determining the COB location along the Iberian margin and Galicia Bank from gravity anomaly inversion, residual depth anomaly and subsidence analysis. *Geophysical Journal International*, **203**, 1355–1372, https://doi.org/10.1093/gji/ggv367

COWIE, L., ANGELO, R.M., KUSZNIR, N.J., MANATSCHAL, G. & HORN, B. 2016. Structure of the ocean–continent transition, location of the continent–ocean boundary and magmatic type of the northern Angolan margin from integrated quantitative analysis of deep seismic reflection and gravity anomaly data. *In*: SABATO CERALDI, T., HODGKINSON, R.A. & BACKE, G. (eds) *Petroleum Geoscience of the West Africa Margin*. Geological Society, London, Special Publications, **438**, 159–176, https://doi.org/10.1144/SP438.6

DIVINS, D.L. 2003. *Total Sediment Thickness of the World's Oceans & Marginal Seas*. NOAA National Geophysical Data Center, Boulder, CO. Updates: http://www.ngdc.noaa.gov/mgg/sedthick/sedthick.html

EDWARDS, R.A., WHITMARSH, R.B. & SCRUTTON, R.A. 1997. The crustal structure across the transform continental margin off Ghana, eastern equatorial Atlantic. *Journal of Geophysical Research*, **102**, 747–772, https://doi.org/10.1029/96JB02098

ELDHOLM, O., GLADCZENKO, T.P., SKOGSEID, J. & PLANKE, S. 2000. Atlantic volcanic margins: a comparative study. *In*: NØTTVEDT, A. (ed) *Dynamics of the Norwegian Margin*. Geological Society, London, Special Publications, **167**, 411–428, https://doi.org/10.1144/GSL.SP.2000.167.01.16

FLETCHER, R.F., KUSZNIR, N.J., ROBERTS, A.M. & HUNSDALE, R. 2013. The formation of a failed continental breakup basin: the Cenozoic development of the Faroe–Shetland Basin. *Basin Research*, **25**, 532–553, https://doi.org/10.1111/bre.12015

FUNCK, T.J., HOPPER, J.R., LARSEN, H.C., LOUDEN, K.E., TUCHOLKE, B.E. & HOLBROOK, W.S. 2003. Crustal structure of the ocean–continent transition at Flemish Cap: seismic refraction results. *Journal of Geophysical Research*, **108**, 2531, https://doi.org/10.1029/2003JB002434

GALLACHER, R.J. & BASTOW, I.D. 2012. The development of magmatism along the Cameroon Volcanic Line: evidence from teleseismic receiver functions. *Tectonics*, **31**, TC3018, https://doi.org/10.1029/2011TC003028

GREENHALGH, E.E. & KUSZNIR, N.J. 2007. Evidence for thin oceanic crust on the extinct Aegir Ridge, Norwegian Basin, NE Atlantic derived from satellite gravity inversion. *Geophysical Research Letters*, **34**, L06305, https://doi.org/10.1029/2007GL029440

GREENROYD, C.J., PEIRCE, C., RODGER, M., WATTS, A.B. & HOBBS, R.W. 2007. Crustal structure of the French Guiana margin, West Equatorial Atlantic. *Geophysical Journal International*, **169**, 964–987, https://doi.org/10.1111/j.1365-246X.2007.03372.x

GREENROYD, C.J., PEIRCE, C., RODGER, M., WATTS, A.B. & HOBBS, R.W. 2008. Demerara Plateau – the structure and evolution of a transform passive margin. *Geophysical Journal International*, **172**, 549–564, https://doi.org/10.1111/j.1365-246X.2007.03662.x

HEKINIAN, R., BONTE, P., DUDLEY, W., BLANC, P.L., JEHANC, C., LABEYRIE, L. & DUPLESSEY, J.C. 1978. Volcanics from the Sierra Leone Rise. *Nature*, **275**, 536–538.

HOPPER, J.R., FUNCK, T. & TUCHOLKE, B.E. 2007. Structure of the Flemish Cap margin, Newfoundland: insights into mantle and crustal processes during continental breakup. *In*: KARNER, G.D., MANATSCHAL, G. & PINHEIRO, L.M. (eds) *Imaging, Mapping, and Modelling Continental Lithosphere Extension and Breakup*. Geological Society, London, Special Publications, **282**, 47–61, https://doi.org/10.1144/SP282.3

KLINGELHOEFER, F., LABAILS, C. *ET AL.* 2009. Crustal structure of the SW-Moroccan margin from wide-angle and reflection seismic data (the DAKHLA experiment) Part A: wide-angle seismic models. *Tectonophysics*, **468**, 63–82, https://doi.org/10.1016/j.tecto.2008.07.022

KUMAR, N. & EMBLEY, R.W. 1977. Evolution and origin of the Ceara Rise: an aseismic rise in the western equatorial Atlantic. Geological Society of America Bulletin, **88**, 683–694.

LASKE, G. & MASTERS, G. 1997. A Global Digital Map of Sediment Thickness. *EOS Transactions, AGU*, **78**, F483. Updates: http://igppweb.ucsd.edu/~gabi/sediment.html

MANATSCHAL, G., LAVIER, L. & CHENIN, P. 2015. The role of inheritance in structuring hyperextended rift systems: some considerations based on observations and numerical modelling. *Gondwana Research*, **27**, 140–164, https://doi.org/10.1016/j.gr.2014.08.006

MCKENZIE, D.P. & BICKLE, M.J. 1988. The volume and composition of melt generated by extension of the lithosphere. *Journal of Petrology*, **29**, 625–679.

MÜLLER, R.D., SDROLIAS, M., GAINA, C. & ROEST, R.W. 2008. Age, spreading rates and spreading symmetry of the world's ocean crust. *Geochemistry Geophysics Geosystems*, **9**, Q04006, https://doi.org/10.1029/2007GC001743, https://www.ngdc.noaa.gov/mgg/ocean_age/ocean_age_2008.html

NEMČOK, M., SINHA, S.T., DORÉ, A.G., LUNDIN, E.R., MASCLE, J. & RYBÁR, S. 2016. Mechanisms of microcontinent release associated with wrenching-involved continental break-up; a review. *In*: NEMČOK, M., RYBÁR, S., SINHA, S.T., HERMESTON, S.A. & LEDVENYIOVA, L. (eds) *Transform Margins: Development, Controls and Petroleum Systems*. Geological Society, London, Special Publications, **431**, 323–359, https://doi.org/10.1144/SP431.14

PINDELL, J.L. & KENNAN, L. 2009. Tectonic evolution of the Gulf of Mexico, Caribbean and northern South America in the mantle reference frame: an update. *In*: JAMES, K.H., LORENTE, M.A. & PINDELL, J.L. (eds) *The Origin and Evolution of the Caribbean Plate*. Geological Society, London, Special Publications, **328**, 1–55, https://doi.org/10.1144/SP328.1

ROBERTS, A.M., KUSZNIR, N.J., CORFIELD, R.I., THOMPSON, M. & WOODFINE, R. 2013. Integrated tectonic basin modelling as an aid to understanding deep-water rifted continental margin structure and location. *Petroleum Geoscience*, **19**, 65–88, https://doi.org/10.1144/petgeo2011-046

SAGE, F., BASILE, Ch., MASCLE, J., PONTOISE, B. & WHITMARSH, R.B. 2000. Crustal structure of the continent–ocean transition off the Côte d'Ivoire–Ghana transform margin: implications for thermal exchanges across the palaeotransfrom boundary. *Geophysical Journal International*, **143**, 662–678.

SANDWELL, D.T. & SMITH, W.H.F. 2009. Global marine gravity from retracked Geosat and ERS-1 altimetry: ridge segmentation v. spreading rate. *Journal of Geophysical Research*, **114**, B01411, https://doi.org/10.1029/2008JB006008, updates http://topex.ucsd.edu/WWW_html/mar_grav.html

SCOTCHMAN, I.C., GILCHRIST, G., KUSZNIR, N.J., ROBERTS, A.M. & FLETCHER, R. 2010. The breakup of the South Atlantic Ocean: formation of failed spreading axes and blocks of thinned continental crust in the Santos basin, Brazil and its consequences for petroleum system development. *In*: VINING, B. & PICKERING, S.C. (eds) *Petroleum Geology: From Mature Basins to New Frontiers – Proceedings of the 7th Petroleum Geology Conference*. Geological Society, London, 855–866, https://doi.org/10.1144/0070855

SETON, M., MÜLLER, R.D. *ET AL.* 2012. Global continental and ocean basin reconstructions since 200 Ma. *Earth-Science Reviews*, **113**, 212–270, https://doi.org/10.1016/j.earscirev.2012.03.002

SMITH, W.H.F. & SANDWELL, D.T. 1997. Global seafloor topography from satellite altimetry and ship depth soundings. *Science*, **277**, 1957–1196. Updates: http://topex.ucsd.edu/marine_topo/

SUTRA, E., MANATSCHAL, G., MOHN, G. & UNTERNEHR, P. 2013. Quantification and restoration of extensional deformation along the Western Iberia and Newfoundland rifted margins. *Geochemistry, Geophysics, Geosystems*, **14**, 2575–2597.

TSIKALAS, F., FALEIDE, J.I., ELDHOLM, O. & WILSON, J. 2005. Late Mesozoic-Cenozoic structural and stratigraphic correlations between the conjugate mid-Norway and NE Greenland continental margins. *In*: DORÉ, A.G. & VINING, B.A. (eds) *Petroleum Geology: North-West Europe and Global Perspectives – Proceedings of the 6th Petroleum Geology Conference*. Geological Society, London, 785–801, https://doi.org/10.1144/0060785

WATTS, A.B., RODGER, M., PEIRCE, C., GREENROYD, C.J. & HOBBS, R.W. 2009. Seismic structure, gravity anomalies, and flexure of the Amazon continental margin, NE Brazil. *Journal of Geophysical Research*, **114**, B07103, https://doi.org/10.1029/2008JB006259

WHITE, R.S. & MCKENZIE, D.P. 1989. Magmatism at rift zones: the generation of volcanic continental margins and flood basalts. *Journal of Geophysical Research*, **94**, 7685–7729.